

Supporting Information

New family of clusters containing a silver-centered tetracapped $[\text{Ag}@\text{Ag}_4(\mu_3-\text{P})_4]$ tetrahedron, inscribed within a N_{12} icosahedron

Alexander V. Artem'ev,^{a*} Irina Yu. Bagryanskaya,^{b,c} Evgeniya P. Doronina,^d Peter M. Tolstoy,^e Artem L. Gushchin,^{a,c} Mariana I. Rakhmanova,^a Alexander Yu. Ivanov,^c Anastasiya O. Suturina^d

^a Nikolaev Institute of Inorganic Chemistry, Siberian Branch of Russian Academy of Sciences, 3, Akad. Lavrentiev Ave., Novosibirsk 630090, Russia

^b N. N. Vorozhtsov Novosibirsk Institute of Organic Chemistry, Siberian Branch of Russian Academy of Sciences, 9, Akad. Lavrentiev Ave., Novosibirsk 630090, Russia

^c Novosibirsk State University, (National Research University), Department of Natural Sciences, 2, Pirogova Str., Novosibirsk 630090, Russia

^d A. E. Favorsky Irkutsk Institute of Chemistry, Siberian Branch of the Russian Academy of Sciences, 1 Favorsky Str., 664033 Irkutsk, Russia

^e St. Petersburg State University, Center for Magnetic Resonance, Universitetskij pr. 26, St.Petersburg 198504, Russia

*Author for correspondence: chemisufarm@yandex.ru (Alexander V. Artem'ev)

Table of Contents

Pages

S2	General remarks
S2-4	Synthesis and characterization data
S4-11	X-Ray crystallography
S12-20	NMR spectra of 1-5
S21-22	FT-IR spectra of 1-5
S23-24	Photophysical measurements
S25	CV measurements

General remarks

All reactions were carried out under an argon atmosphere. Tris(2-pyridyl)phosphine was synthesized from red phosphorus and 2-bromopyridine according to the published method.^[1] AgOTf, Ag(MeCN)₄]BF₄, [Ag(MeCN)₄]PF₆ and AgNO₃ were used as purchased. Acetonitrile was HPLC grade (Sigma-Aldrich). Dichloromethane was purified following standard procedure.

Elemental analyses for C, N, and H were performed on a Flash EA 1112 CHNS elemental analyzer. The ¹H, ³¹P{¹H}, ¹⁰⁹Ag and constant time ¹H, ¹⁵N-HMBC NMR spectra were recorded at room temperature on a Bruker AV-400 and Bruker Avance III 400 (Center for Magnetic Resonance, SPbU Research Park) spectrometers (400.13 MHz for ¹H, 161.97 MHz for ³¹P, 40.55 MHz for ¹⁵N, 18.63 for ¹⁰⁹Ag). The NMR spectra were referenced through the solvent lock (²H) signal according to IUPAC recommended secondary referencing method. The ¹H, ³¹P, ¹⁵N and ¹⁰⁹Ag NMR chemical shifts are reported in the scales of tetramethylsilane, 85% H₃PO₄ in D₂O, liq. NH₃ and AgNO₃ (sat.) in D₂O as standards, respectively. The number of scans was 16 for ¹H (2 s pulse delay delay), 256 for ³¹P (3 s pulse delay) and 10k for ¹⁰⁹Ag (30 s pulse delay). ¹H, ¹⁵N-HMBC spectra were recorded using 2048x32 points, 8 scans and 2 s pulse delay. High-resolution constant-time ¹H, ¹⁵N-HMBC spectrum given in the main text was adjusted to the NH coupling constant of 9 Hz. Deuterated solvents (CD₃CN, *Deutero GmbH*; D₂O, *abcr GmbH*) were used without further purification. The coupling constants (*J*) are given in Hertz. The IR spectra were recorded on a Varian 3100 FT-IR spectrometer with ATR sample setting. Melting points were determined with a Kofler micro hot stage.

Synthesis and characterization data

Complex 1

To a stirred solution of AgOTf (188 mg, 0.73 mmol) in acetonitrile (1 mL), a solution of Py₃P (155 mg, 0.58 mmol) in dichloromethane (8 mL) was added. Immediately, a white precipitate was formed. The resulting suspension was stirred for 1 h at room temperature. The white precipitate was collected by centrifugation, washed with dichloromethane (1 × 3 mL) and dried in vacuum.

Yield: 288 mg (84%). White powder, decomposed without melting (*ca.* 252-254 °C). ¹H NMR (400.13 MHz, CD₃CN, ppm), δ : 8.24 (d, $^3J_{HH}$ = 4.2 Hz, 12H, H-6), 7.87 (t, $^3J_{HH}$ = 7.8 Hz, 12H, H-4), 7.39 (t, $^3J_{HH}$ = 6.4 Hz, 12H, H-5), 6.61 (d, $^3J_{HH}$ = 7.8 Hz, 12H, H-3). ³¹P{¹H} NMR (161.98 MHz, CD₃CN, ppm), δ : 14.63 (d, $^1J_{Ag-P}$ = 222.8 Hz, ¹⁰⁷Ag/¹⁰⁹Ag average). ¹⁰⁹Ag NMR (18.63 MHz, CD₃CN, ppm), δ : 671.25. FT-IR (ATR): ν = 571 (m), 633 (vs), 741 (m), 764 (s), 903 (w), 1007 (s), 1026 (s), 1053 (w), 1096 (m), 1150 (s), 1223 (s), 1242 (s), 1273 (m), 1431 (m), 1454 (m), 1566 (w), 1578 (m), 1647 (w), 1736 (vw), 1879 (vw), 2095 (w), 2257 (vw), 2291 (vw), 2488 (vw), 2581 (vw), 2743 (vw), 2855 (vw), 2924 (vw), 3005 (w), 3086

^[1] B. A. Trofimov, A. V. Artem'ev, S. F. Malysheva, N. K. Gusarova, N. A. Belogorlova, A. O. Korocheva, Yu. V. Gatilov, V. I. Mamatyuk, *Tetrahedron Lett.* **2012**, 53, 2424.

(w) cm^{-1} . Anal. Calcd for $\text{C}_{65}\text{H}_{48}\text{Ag}_5\text{F}_{15}\text{N}_{12}\text{O}_{15}\text{P}_4\text{S}_5$: C, 33.28; H, 2.06; N, 7.17. Found: C, 33.05; H, 2.19; N, 6.88.

Complex 2

To a stirred solution of $[\text{Ag}(\text{MeCN})_4]\text{BF}_4$ (200 mg, 0.56 mmol) in acetonitrile (1.5 mL), a solution of Py_3P (118 mg, 0.44 mmol) in dichloromethane (8 mL) was added. Immediately, a white precipitate was formed. The resulting suspension was stirred for 1 h at room temperature. The white precipitate was collected by centrifugation, washed with dichloromethane (1×3 mL) and dried in vacuum.

Yield: 224 mg (99%). White powder, decomposed without melting (*ca.* 230 °C). ^1H NMR (400.13 MHz, CD_3CN , ppm), δ : 8.22 (d, $^3J_{\text{HH}} = 4.7$ Hz, 12H, H-6), 7.87 (t, $^3J_{\text{HH}} = 7.8$ Hz, 12H, H-4), 7.40 (t, $^3J_{\text{HH}} = 6.5$ Hz, 12H, H-5), 6.61 (d, $^3J_{\text{HH}} = 7.8$ Hz, 12H, H-3). $^{31}\text{P}\{\text{H}\}$ NMR (161.98 MHz, CD_3CN , ppm), δ : 14.75 (d, $^1J_{\text{Ag-P}} = 222.3$ Hz, $^{107}\text{Ag}/^{109}\text{Ag}$ average). ^{109}Ag NMR (18.63 MHz, CD_3CN , ppm), δ : 674.15. FT-IR (ATR): $\nu = 576$ (m), 616 (vw), 634 (w), 669 (w), 726 (w), 741 (m), 762 (s), 841 (vw), 905 (w), 1005 (vs), 1036 (vs), 1048 (vs), 1059 (vs), 1169 (w), 1291 (w), 1430 (m), 1457 (m), 1579 (m), 2887 (vw), 3099 (w) cm^{-1} . Anal. Calcd for $\text{C}_{60}\text{H}_{48}\text{Ag}_5\text{B}_5\text{F}_{20}\text{N}_{12}\text{P}_4$: C, 35.42; H, 2.38; N, 8.26. Found: C, 35.18; H, 2.46; N, 8.01.

Complex 3

To a mixture of $[\text{Ag}(\text{MeCN})_4]\text{PF}_6$ (190 mg, 0.45 mmol) and Py_3P (97 mg, 0.36 mmol), dichloromethane (5 mL) was added. The mixture was stirred for 1 h at room temperature. The formed precipitate was collected by centrifugation, washed with dichloromethane (1×3 mL) and dried in vacuum.

Yield: 183 mg (86%). White powder, > 240 °C dec. ^1H NMR (400.13 MHz, CD_3CN , ppm), δ : 8.19 (d, $^3J_{\text{HH}} = 4.9$ Hz, 12H, H-6), 7.85 (t, $^3J_{\text{HH}} = 7.8$ Hz, 12H, H-4), 7.38 (t, $^3J_{\text{HH}} = 6.3$ Hz, 12H, H-5), 6.59 (d, $^3J_{\text{HH}} = 7.8$ Hz, 12H, H-3). $^{31}\text{P}\{\text{H}\}$ NMR (161.98 MHz, CD_3CN , ppm), δ : 14.72 (d, $^1J_{\text{Ag-P}} = 224.2$ Hz, $^{107}\text{Ag}/^{109}\text{Ag}$ average). ^{109}Ag NMR (18.63 MHz, CD_3CN , ppm), δ : 674.20. FT-IR (ATR): $\nu = 555$ (m), 633 (w), 706 (m), 737 (s), 760 (s), 837 (vs), 880 (m), 1007 (s), 1061 (m), 1126 (w), 1169 (w), 1246 (w), 1292 (w), 1377 (w), 1431 (m), 1454 (m), 1566 (w), 1578 (m), 1636 (w), 1748 (vw), 1802 (vw), 1879 (vw), 1983 (w), 2014 (w), 2257 (w), 2295 (w), 2338 (vw), 2419 (vw), 2492 (w), 2581 (vw), 2677 (vw), 2743 (vw), 2947 (vw), 3005 (w), 3090 (w), 3568 (w) cm^{-1} . Anal. Calcd for $\text{C}_{60}\text{H}_{48}\text{Ag}_5\text{F}_{30}\text{N}_{12}\text{P}_9$: C, 30.99; H, 2.08; N, 7.23. Found: C, 30.65; H, 1.87; N, 7.14.

Complex 4

To a stirred solution of $[\text{Ag}(\text{MeCN})_4]\text{BF}_4$ (69 mg, 0.192 mmol) and $[\text{Ag}(\text{MeCN})_4]\text{PF}_6$ (20 mg, 0.048 mmol) in acetonitrile (1.5 mL), a solution of Py_3P (51 mg, 0.192 mmol) in dichloromethane (8 mL) was added. Immediately, a white precipitate was formed. The resulting suspension was stirred for 1 h at room temperature. The white precipitate was collected by centrifugation, washed with dichloromethane (1×3 mL) and dried in vacuum.

Yield: 85 mg (85%). White powder, decomposed without melting (*ca.* 230 °C). ^1H NMR (400.13 MHz, CD₃CN, ppm), δ : 8.23 (d, $^3J_{\text{HH}} = 5.1$ Hz, 12H, H-6), 7.88 (t, $^3J_{\text{HH}} = 7.7$ Hz, 12H, H-4), 7.41 (t, $^3J_{\text{HH}} = 6.1$ Hz, 12H, H-5), 6.63 (d, $^3J_{\text{HH}} = 7.9$ Hz, 12H, H-3). $^{31}\text{P}\{\text{H}\}$ NMR (161.98 MHz, CD₃CN, ppm), δ : 14.73 (d, $^1J_{\text{Ag-P}} = 222.3$ Hz, $^{107}\text{Ag}/^{109}\text{Ag}$ average). ^{109}Ag NMR (18.63 MHz, CD₃CN, ppm), δ : 672.94. FT-IR (ATR): $\nu = 401$ (m), 417 (m), 447 (s), 482 (s), 500 (vs), 511 (vs), 557 (s), 633 (m), 727 (s), 739 (s), 764 (vs), 843 (vs), 878 (m), 1007 (vs), 1069 (vs), 1246 (w), 1290 (m), 1431 (s), 1456 (s), 1566 (m), 1580 (s), 1636 (w), 3005 (m), 3098 (m), 3136 (m), 3161 (m) cm⁻¹. Anal. Calcd for C₆₀H₄₈Ag₅B₄F₂₂N₁₂P₅: C, 34.44; H, 2.31; N, 8.03. Found: C, 34.09; H, 2.41; N, 7.79.

Complex 5 (Optimized procedure)

To a mixture of AgCl (110 mg, 0.77 mmol) and Py₃P (244 mg, 0.92 mmol), MeCN (5 mL) was added. The resulting suspension was stirred for 1 h at room temperature. The formed precipitate was collected by centrifugation, washed with dichloromethane (1 × 10 mL) and dried in vacuum. The similar complex was isolated, when the AgCl and Py₃P were taken in the 5:4 molar ratio, respectively.

Yield: 298 mg (95%). White powder, poor soluble in organic solvents. ^1H NMR (400.13 MHz, CD₃CN, ppm), δ : 8.36 (d, $^3J_{\text{HH}} = 4.7$ Hz, 6H, H-6), 7.94 (t, $^3J_{\text{HH}} = 7.7$ Hz, 6H, H-4), 7.46 – 7.41 (t, $^3J_{\text{HH}} = 6.0$ Hz, 6H, H-5), 6.72 (d, $^3J_{\text{HH}} = 7.8$ Hz, 6H, H-3). $^{31}\text{P}\{\text{H}\}$ NMR (161.98 MHz, CD₃CN, ppm), δ : 15.44 (d, $^1J_{\text{Ag-P}} = 213.8$ Hz, $^{107}\text{Ag}/^{109}\text{Ag}$ average). Anal. Calcd for C₃₀H₂₄Ag₂Cl₂N₆P₂: C, 44.10; H, 2.96; N, 10.28. Found: C, 44.01; H, 3.12; N, 10.04.

X-Ray crystallography

The single crystals of **1**·4Me₂CO were obtained by liquid diffusion of hexane into an acetone solution of **1** at r.t. The single crystals of **2**·Me₂CO·2.5MeCN were growing by liquid diffusion of hexane into a solution of **2** in acetone/acetonitrile mixture. The single crystals of **3**·MeCN and **4**·6MeCN were growing by vapor diffusion of diethyl ether into an acetonitrile solution of **3** or **4**. The colorless crystals of **1**·4Me₂CO, **3**·MeCN and **4**·6MeCN, upon removal from the supernatant solution, quickly become matt due to the fast losing of the solvent molecules. The single crystals of **5**·3CHCl₃ were obtained by a slow liquid diffusion of hexane into a chloroform solution of **5** at r.t.

X-Ray crystallographic study of the crystals were carried out on a Bruker Kappa Apex II CCD diffractometer using φ, ω -scans of narrow (0.5°) frames with MoK α radiation ($\lambda = 0.71073$ Å) and a graphite monochromator. The structures were solved by direct methods SHELXL97^[2] and refined by a full matrix least-squares anisotropic-isotropic (for H atom) procedure using SHELXL-2014/7^[3] programs set.

^[2] G. M. Sheldrick, SHELX-97, Programs for Crystal Structure Analysis (Release 97-2), University of Göttingen, Germany, 1997.

^[3] G. M. Sheldrick, Acta Cryst., **2015**, C71, 3-8.

Absorption corrections were applied using the empirical multiscan method with the SADABS program.^[4] The positions of the hydrogen atoms were calculated with the riding model. In the crystals of **3**·MeCN, only the part of solvent molecules has been located. Free solvent accessible volume derived from PLATON^[5] routine analysis was found to be 29.1 % (3009.0 Å³). This **5**·3CHCl₃ was refined as a 0.66 : 0.34 racemic twin. This volume is occupied by highly disordered solvent molecules that could not be modeled as a set of discrete atomic sites. We employed PLATON/SQUEEZE^[6] procedure to calculate the contribution to the diffraction from the solvent region and thereby produced a set of solvent-free diffraction intensities. In the crystal packing of **1**·4Me₂CO, one of the triflate anion is strong disordered, so the all atoms in this anion except atoms S have been refined by isotropic. The obtained crystal structures were analyzed for short contacts between non-bonded atoms using PLATON^[5] and MERCURY programs.^[6]

Crystallographic data of the structures **1**–**5** are listed in Table S1. CCDC 1472281 (**1**), 1472282 (**2**), 1532341 (**3**), 1538903 (**4**) and 1552867 (**5**) contain the supplementary crystallographic data for this paper. These data can be obtained from the Cambridge Crystallographic Data Centre via www.ccdc.cam.ac.uk/data_request/cif.

Table S1. Data collection and refinement parameters for **1**–**5**.

Compound	1 ·4Me ₂ CO	2 ·Me ₂ CO·2.5MeCN	3 ·MeCN	4 ·6MeCN	5 ·3CHCl ₃
Empirical formula	C ₆₅ H ₄₈ Ag ₅ F ₁₅ N ₁₂ O ₁₅ P ₄ S ₅	C ₆₉ H _{61.5} Ag ₅ B ₅ F ₂₀ N ₁₅ OP ₄	C ₆₂ H ₄₉ Ag ₅ F ₃₀ N ₁₃ P ₉	C ₇₂ H ₆₆ Ag ₅ B ₄ F ₂₂ N ₁₈ P ₅	2(C ₃₀ H ₂₄ Ag ₂ Cl ₂ N ₆ P ₂)·5CHCl ₃
Formula mass [g/mol]	2345.69	2214.11	2364.22	2338.87	2231.17
Space group	P2 ₁ /n	P2 ₁ /n	P2 ₁ /n	P-1	P2 ₁
<i>a</i> [Å]	16.4246(7)	23.685(3)	18.482(2)	14.3371(6)	17.3997(16)
<i>b</i> [Å]	22.9762(11)	22.865(2)	22.800(3)	14.4204(5)	16.0691(15)
<i>c</i> [Å]	28.4848(11)	30.599(3)	24.670(4)	22.4241(9)	17.4938(15)
α [°]	90.00	90.00	90.00	84.0450(10)	90.00
β [°]	105.155(2)	90.970(4)	96.390(6)	87.7610(10)	110.354(4)
γ [°]	90.00	90.00	90.00	69.1570(10)	90.00
<i>V</i> [Å ³]	10375.6(8)	16568(3)	10331(3)	4309.3(3)	4585.8(7)
<i>Z</i>	4	8	4	2	12
<i>D</i> _{calcd.} [g·cm ⁻³]	1.554	1.775	1.520	1.803	1.616
μ [mm ⁻¹]	1.151	1.336	1.163	1.310	1.508
Temperature [K]	200(2)	200(2)	296(2)	200(2)	296(2)
Reflections collected	105177	245571	43774	87103	82279
Independent reflections	27225 [<i>R</i> _{int} = 0.0336]	38073 [<i>R</i> _{int} = 0.0543]	16985 [<i>R</i> _{int} = 0.0748]	19773 [<i>R</i> _{int} = 0.0293]	16157 [<i>R</i> _{int} = 0.0267]
<i>R</i> ₁ , <i>wR</i> ₂ [<i>I</i> > 2σ(<i>I</i>)]	0.0614, 0.1678	0.0399, 0.1145	0.0873, 0.2360	0.0419, 0.1147	0.0549, 0.1598
<i>R</i> ₁ , <i>wR</i> ₂ (all data)	0.1029, 0.1792	0.0535, 0.1215	0.1500, 0.2589	0.0630, 0.1393	0.0675, 0.1783
Goodness of fit	1.165	1.097	1.047	1.031	1.067
Largest diff peak and hole [e·Å ⁻³]	3.11 and -1.88	1.67 and -1.42	2.20 and -1.82	2.32 and -0.91	1.56 and -0.61

^[4] SADABS, v. 2008-1, Bruker AXS, Madison, WI, USA, 2008.

^[5] (a) A. L. Spek, PLATON, A Multipurpose Crystallographic Tool (Version 10M), Utrecht University, Utrecht, The Netherlands, 2003; (b) A. L. Spek, *J. Appl. Crystallogr.* **2003**, *36*, 7–13.

^[6] C. F. Macrae, P. R. Edgington, P. McCabe, E. Pidcock, G. P. Shields, R. Taylor, M. Towler, J. van de Stree, *J. Appl. Crystallogr.* **2006**, *39*, 453–457.

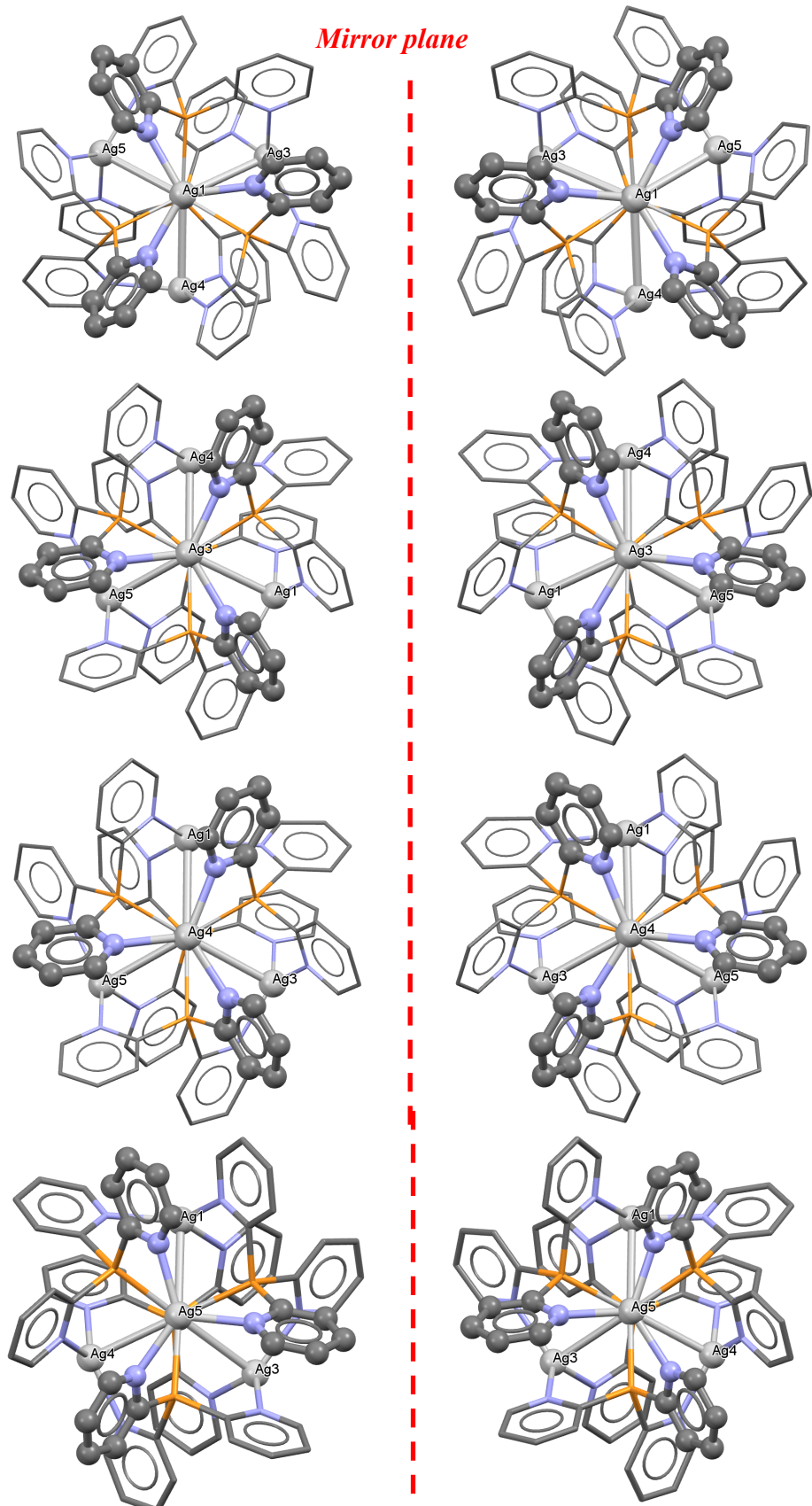
Table S2. Selected bond lengths, bond angles and torsion angles for **1–5**.

Complex 1			
Ag1–N7	2.272(5)		
Ag1–N12	2.301(5)		
Ag1–N11	2.300(5)		
Ag1–Ag2	3.1622(6)		
Ag2–P4	2.5766(16)	P4–Ag2–P1	109.44(5)
Ag2–P1	2.5849(16)	P4–Ag2–P3	108.91(5)
Ag2–P3	2.6029(15)	P1–Ag2–P3	109.86(5)
Ag2–P2	2.6095(15)	P4–Ag2–P2	108.45(5)
Ag2–Ag4	3.0917(7)	P1–Ag2–P2	109.21(5)
Ag2–Ag5	3.1313(6)	P3–Ag2–P2	110.94(5)
Ag2–Ag3	3.1638(6)	Ag4–Ag2–Ag5	107.983(18)
Ag3–N9	2.279(5)	Ag4–Ag2–Ag1	106.253(17)
Ag3–N8	2.286(5)	Ag5–Ag2–Ag1	111.895(17)
Ag3–N1	2.288(5)	Ag4–Ag2–Ag3	107.312(17)
Ag4–N3	2.279(5)	Ag5–Ag2–Ag3	113.194(18)
Ag4–N2	2.286(5)	Ag1–Ag2–Ag3	109.842(17)
Ag4–N6	2.306(5)		
Ag5–N4	2.278(5)		
Ag5–N5	2.277(5)		
Ag5–N10	2.303(5)		
Ag5–O1	2.571(6)		
Complex 2			
Ag1–N4	2.282(3)		
Ag1–N1	2.296(3)		
Ag1–N11	2.316(3)		
Ag1–Ag2	3.1451(4)		
Ag2–P1	2.5650(10)		
Ag2–P3	2.5841(10)	P1–Ag2–P3	109.05(3)
Ag2–P2	2.5905(9)	P1–Ag2–P2	111.27(3)
Ag2–P4	2.5961(9)	P3–Ag2–P2	109.02(3)
Ag2–Ag4	3.0880(5)	P1–Ag2–P4	109.32(3)
Ag2–Ag3	3.1355(4)	P3–Ag2–P4	110.57(3)
Ag2–Ag5	3.1444(4)	P2–Ag2–P4	107.61(3)
Ag3–N2	2.311(3)	Ag4–Ag2–Ag3	106.669(13)
Ag3–N3	2.324(3)	Ag4–Ag2–Ag5	109.385(13)
Ag3–N7	2.328(3)	Ag3–Ag2–Ag5	110.075(13)
Ag3–N1A	2.435(4)	Ag4–Ag2–Ag1	112.434(13)
Ag4–N6	2.278(3)	Ag3–Ag2–Ag1	107.885(13)
Ag4–N5	2.282(3)	Ag5–Ag2–Ag1	110.309(13)
Ag4–N12	2.287(3)		
Ag5–N9	2.307(3)		
Ag5–N10	2.312(3)		
Ag5–N8	2.313(3)		
Ag5–N2A	2.546(4)		

Complex 3			
Ag1–Ag2	3.2182(10)		
Ag2–Ag5	3.1477(11)		
Ag2–Ag3	3.1603(10)		
Ag2–Ag4	3.2131(10)		
Ag1–Ag4	5.3100(11)		
Ag3–Ag4	5.2432(11)		
Ag1–Ag3	5.1872(11)		
Ag1–Ag5	5.1597(12)		
Ag3–Ag5	5.0980(13)		
Ag2–P4	2.581(2)		
Ag2–P2	2.589(2)		
Ag2–P3	2.592(3)		
Ag2–P1	2.598(2)		
Ag1–N2	2.286(7)	Ag3–Ag2–Ag4	110.70(3)
Ag1–N8	2.294(7)	Ag3–Ag2–Ag1	108.82(3)
Ag1–N14	2.328(8)	Ag4–Ag2–Ag1	111.31(3)
Ag3–N3	2.292(6)	Ag5–Ag2–Ag1	108.29(3)
Ag3–N4	2.309(7)	Ag5–Ag2–Ag3	107.83(3)
Ag3–N9	2.312(7)	Ag5–Ag2–Ag4	109.79(3)
Ag3–N13	2.497(10)	P4–Ag2–P2	110.25(7)
Ag4–N6	2.300(7)	P4–Ag2–P3	108.07(8)
Ag4–N10	2.297(8)	P2–Ag2–P3	109.56(7)
Ag4–N7	2.309(8)	P4–Ag2–P1	109.58(7)
Ag5–N5	2.309(8)	P2–Ag2–P1	109.55(7)
Ag5–N12	2.325(7)	P3–Ag2–P1	109.81(8)
Ag5–N11	2.329(7)	C55–N13–Ag3	174.8(11)
Ag1–N2	2.286(7)		
Ag1–N8	2.294(7)		
Ag1–N14	2.328(8)		
Ag3–N3	2.292(6)		
Ag3–N4	2.309(7)		
Ag3–N9	2.312(7)		
Ag3–N13	2.497(10)		
Ag4–N6	2.300(7)		
Ag4–N10	2.297(8)		
Ag4–N7	2.309(8)		
Ag5–N5	2.309(8)		
Ag5–N12	2.325(7)		
Ag5–N11	2.329(7)		
Complex 4			
Ag1–Ag2	3.2233(5)	Ag3–Ag2–Ag1	109.115(12)
Ag1–N1	2.287(4)	Ag4–Ag2–Ag1	111.420(13)
Ag1–N2	2.295(4)	Ag4–Ag2–Ag3	109.233(13)
Ag1–N13	2.287(4)	Ag4–Ag2–Ag5	108.139(13)
Ag2–Ag3	3.1784(5)	Ag5–Ag2–Ag1	110.944(13)

Ag2–Ag4	3.1098(5)	Ag5–Ag2–Ag3	107.910(13)
Ag2–Ag5	3.1672(5)	P1–Ag2–P3	108.65(4)
Ag2–P1	2.5767(11)	P1–Ag2–P4	111.50(4)
Ag2–P2	2.5672(11)	P2–Ag2–P1	108.40(4)
Ag2–P3	2.5790(11)	P2–Ag2–P3	109.48(3)
Ag2–P4	2.5958(11)	P2–Ag2–P4	108.89(4)
Ag3–N3	2.299(4)		
Ag3–N4	2.289(4)		
Ag3–N7	2.288(4)		
Ag3–N14	2.628(5)		
Ag4–N5	2.292(4)		
Ag4–N6	2.281(4)		
Ag4–N12	2.300(4)		
Ag4–N20	2.509(5)		
Ag5–N8	2.290(4)		
Ag5–N9	2.302(4)		
Ag5–N10	2.302(4)		
Ag5–N11	2.599(5)		
<hr/>			
Ag1–Ag2	3.2612(8)	P1–Ag1–N1	129.74(17)
Ag3–Ag4	3.2710(9)	P1–Ag1–N2	128.60(19)
Ag1–P1	2.3823(17)	N1–Ag1–N2	84.0(2)
Ag1–N1	2.388(6)	P1–Ag1–Cl1	116.37(8)
Ag1–N2	2.401(7)	N1–Ag1–Cl1	93.98(17)
Ag1–Cl1	2.597(2)	N2–Ag1–Cl1	94.09(18)
Ag2–P2	2.3807(17)	P1–Ag1–Ag2	71.26(6)
Ag2–N5	2.380(7)	N1–Ag1–Ag2	81.03(16)
Ag2–N4	2.388(7)	N2–Ag1–Ag2	79.61(17)
Ag2–Cl2	2.576(2)	Cl1–Ag1–Ag2	172.29(5)
Ag3–N8	2.360(7)	P2–Ag2–N5	128.60(18)
Ag3–P4	2.373(2)	P2–Ag2–N4	128.95(18)
Ag3–N7	2.369(7)	N5–Ag2–N4	84.0(2)
Ag3–Cl3	2.574(2)	P2–Ag2–Cl2	116.96(8)
Ag3–Ag4	3.2710(9)	N5–Ag2–Cl2	92.3(2)
Ag4–N11	2.376(7)	N4–Ag2–Cl2	95.9(2)
Ag4–P3	2.3916(19)	P2–Ag2–Ag1	70.89(5)
Ag4–N10	2.440(8)	N5–Ag2–Ag1	79.88(19)
Ag4–Cl4	2.595(2)	N4–Ag2–Ag1	80.2(2)
		Cl2–Ag2–Ag1	171.60(6)

Figure S1. The comparison of the configuration for each stereocenter (Ag1, Ag3, Ag4 and Ag5) of $\Delta\Delta\Delta\Delta$ - and $\Lambda\Lambda\Lambda\Lambda$ -enantiomers of **1**.



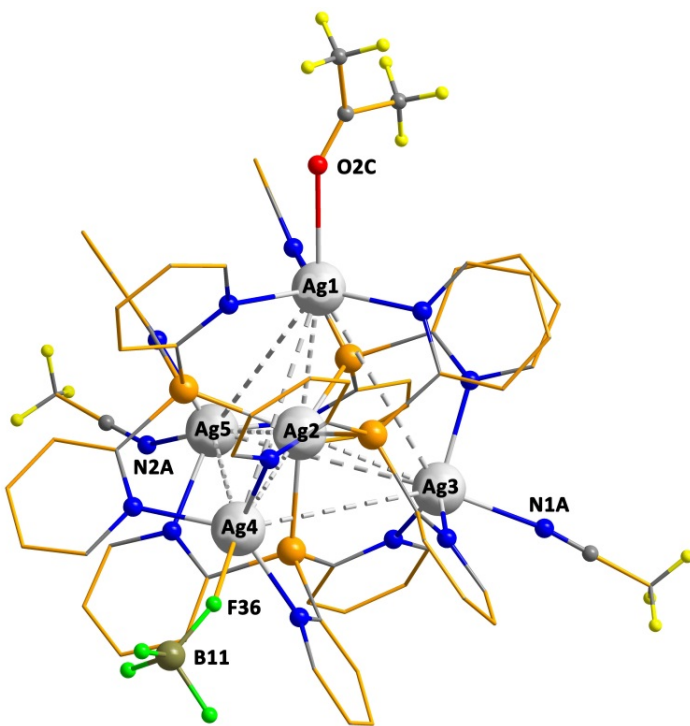


Figure S2. Structure of $[\text{Ag}@\text{Ag}_4(\text{Py}_3\text{P})_4(\text{Me}_2\text{CO})(\text{MeCN})_2]^{5+}$ cation of $\mathbf{2}\cdot\text{Me}_2\text{CO}\cdot2.5\text{MeCN}$ associated with BF_4^- anion (the pyridine H atoms are omitted for clarity).

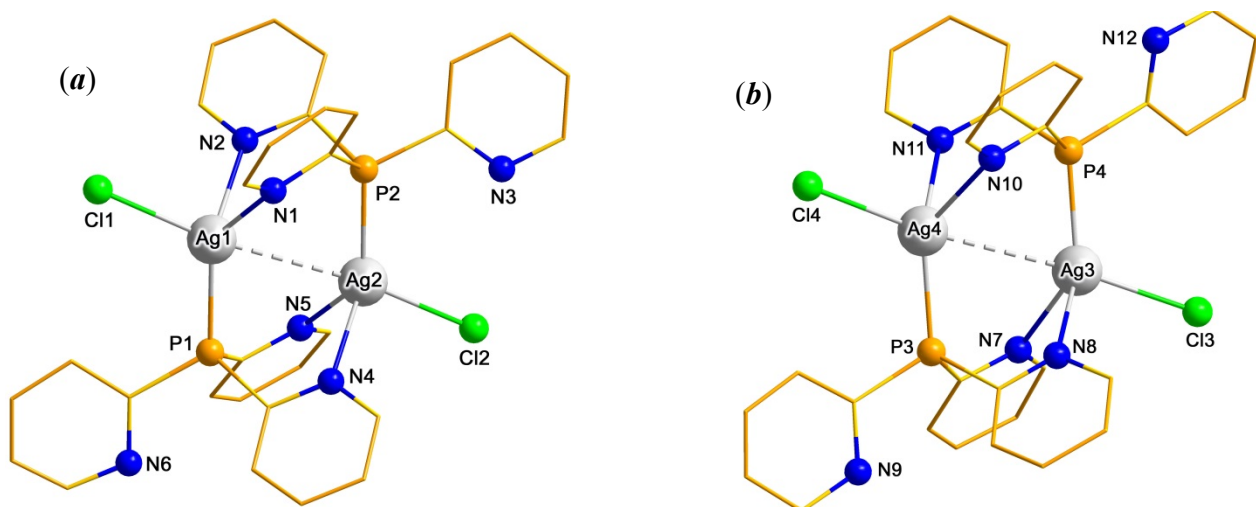


Figure S3. Molecular structures of two independent molecules (**a** and **b**) in crystal of $\mathbf{5}\cdot3\text{CHCl}_3$ (the H atoms are omitted for clarity).

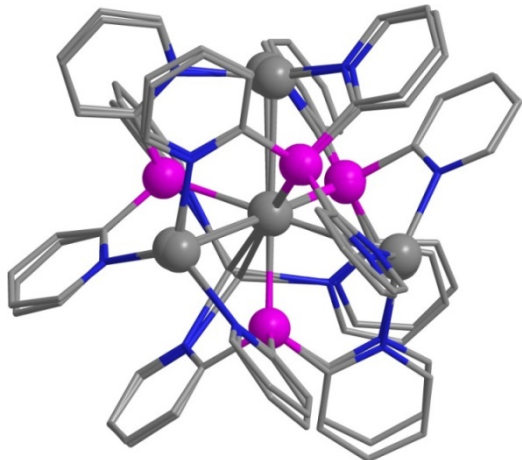


Figure S4. Overlay of the $[\text{Ag}@\text{Ag}_4(\text{Py}_3\text{P})_4]$ skeletons of **1**·4Me₂CO and **2**·Me₂CO·2.5MeCN (the pyridine H atoms are omitted for clarity).

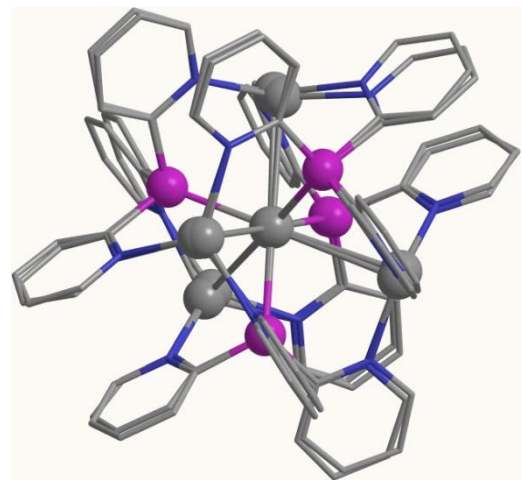


Figure S5. Overlay of the $[\text{Ag}@\text{Ag}_4(\text{Py}_3\text{P})_4]$ skeletons of **1**·4Me₂CO and **3**·MeCN (the pyridine H atoms are omitted for clarity).

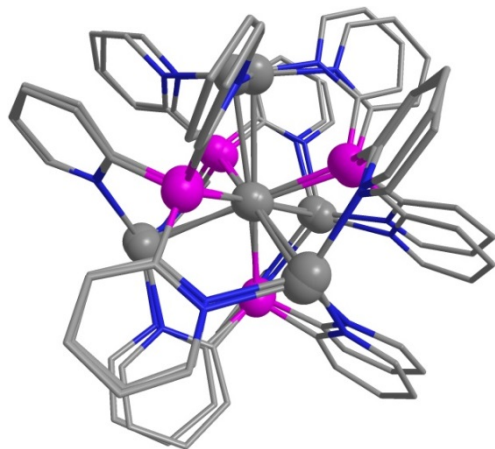


Figure S6. Overlay of the $[\text{Ag}@\text{Ag}_4(\text{Py}_3\text{P})_4]$ skeletons of **4**·6MeCN and **1** (the pyridine H atoms are omitted for clarity).

NMR spectra of the synthesized compounds 1-5

Figure S7. ^1H NMR spectrum of **1** dissolved in CD_3CN at room temperature (selected range).

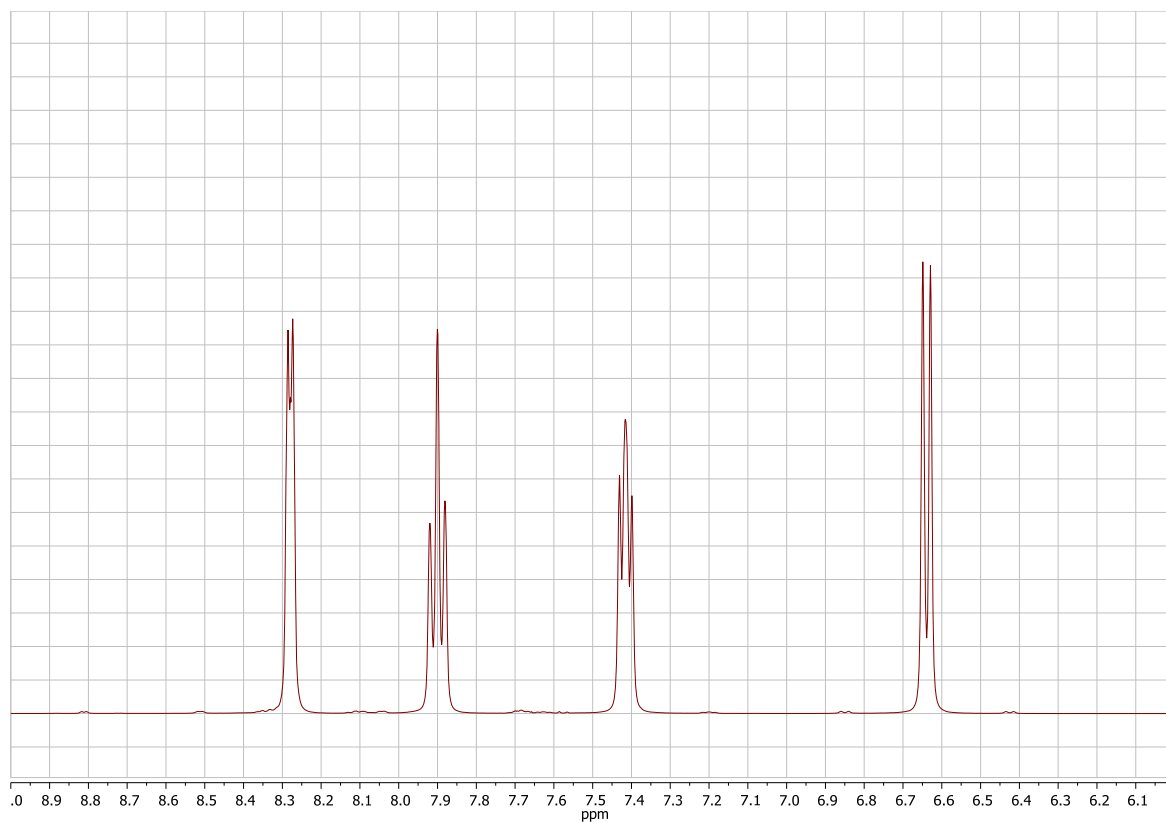


Figure S8. $^{31}\text{P}\{^1\text{H}\}$ NMR spectrum of **1** dissolved in CD_3CN at room temperature (selected range).

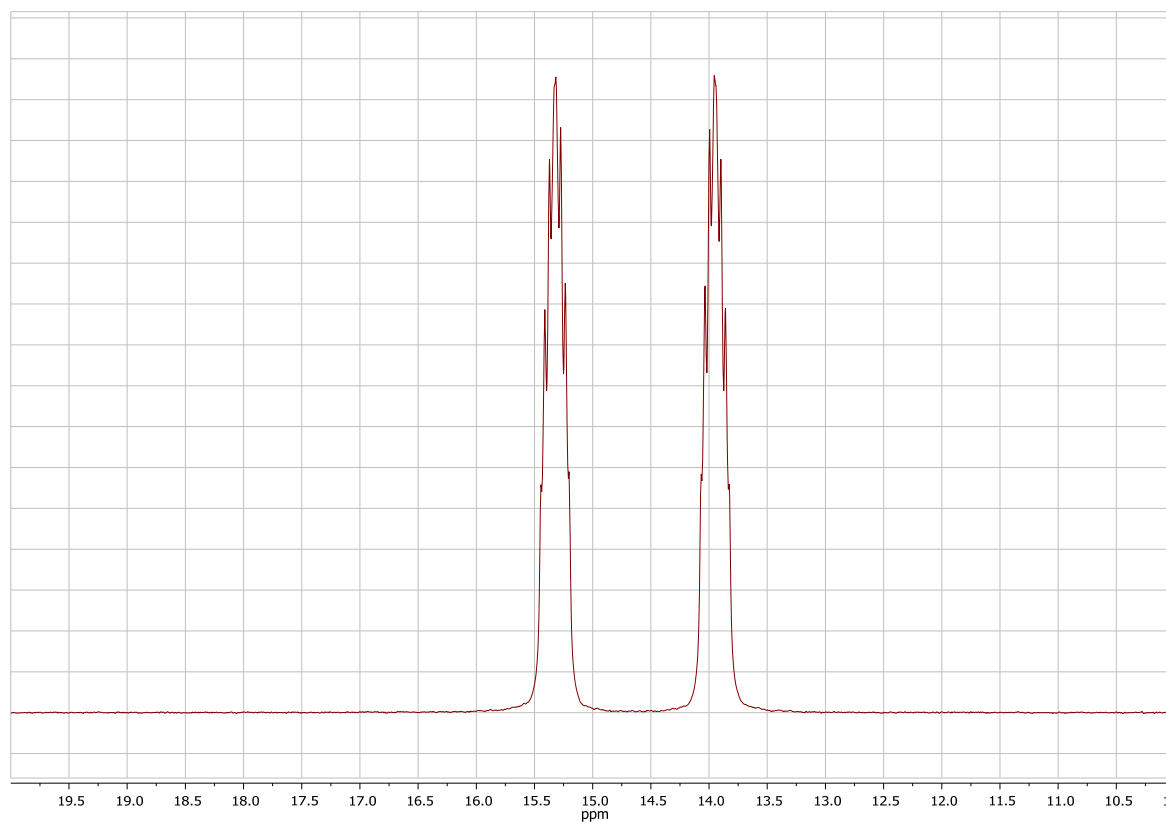


Figure S9. ^{109}Ag NMR spectrum of **1** dissolved in CD_3CN at room temperature (selected range).

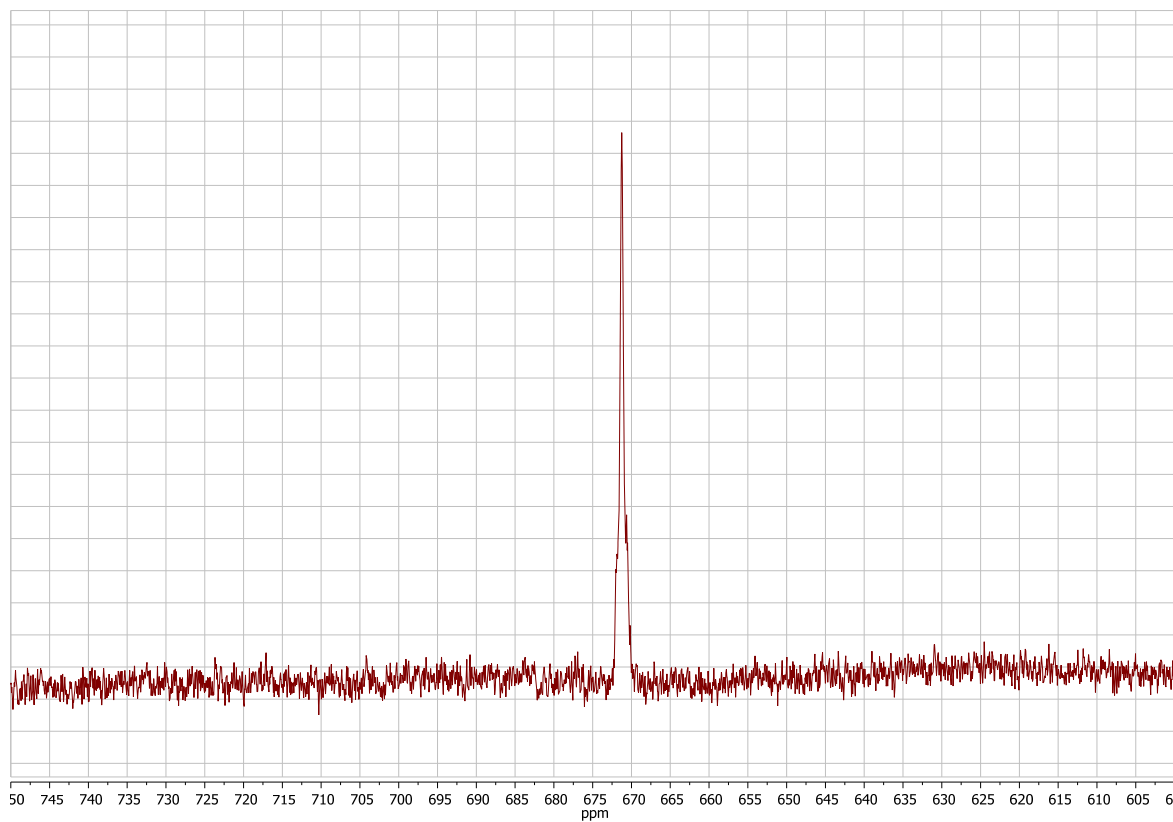


Figure S10. $^1\text{H}, ^{15}\text{N}$ -HMBC NMR spectrum of **1** dissolved in CD_3CN at room temperature (selected range).

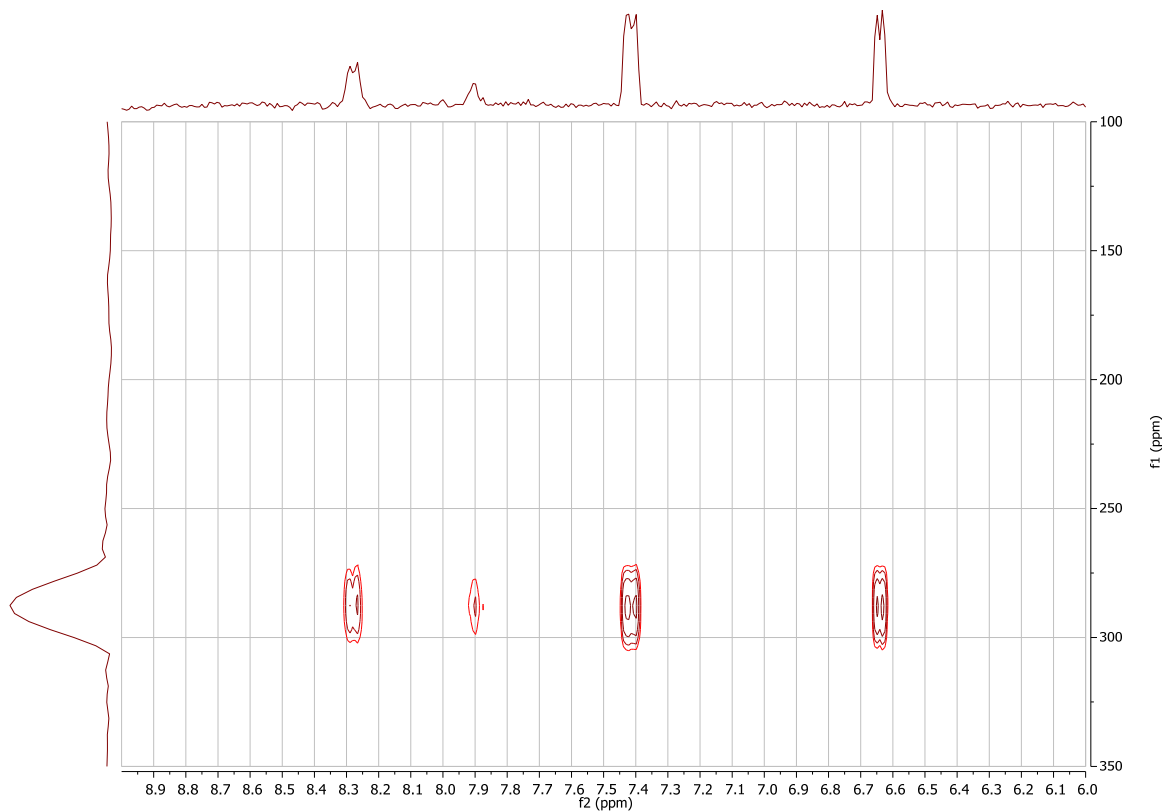


Figure S11. ^1H NMR spectrum of **2** dissolved in CD_3CN at room temperature (selected range).

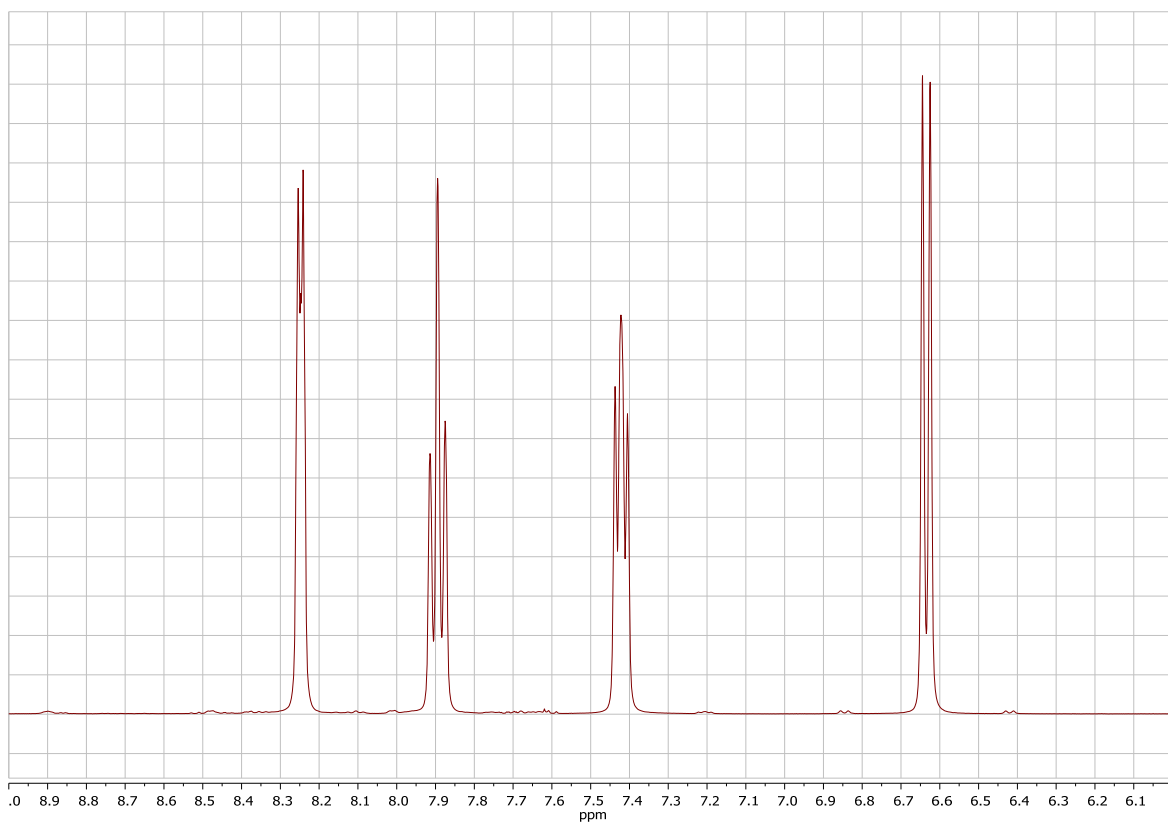


Figure S12. $^{31}\text{P}\{^1\text{H}\}$ NMR spectrum of **2** dissolved in CD_3CN at room temperature (selected range).

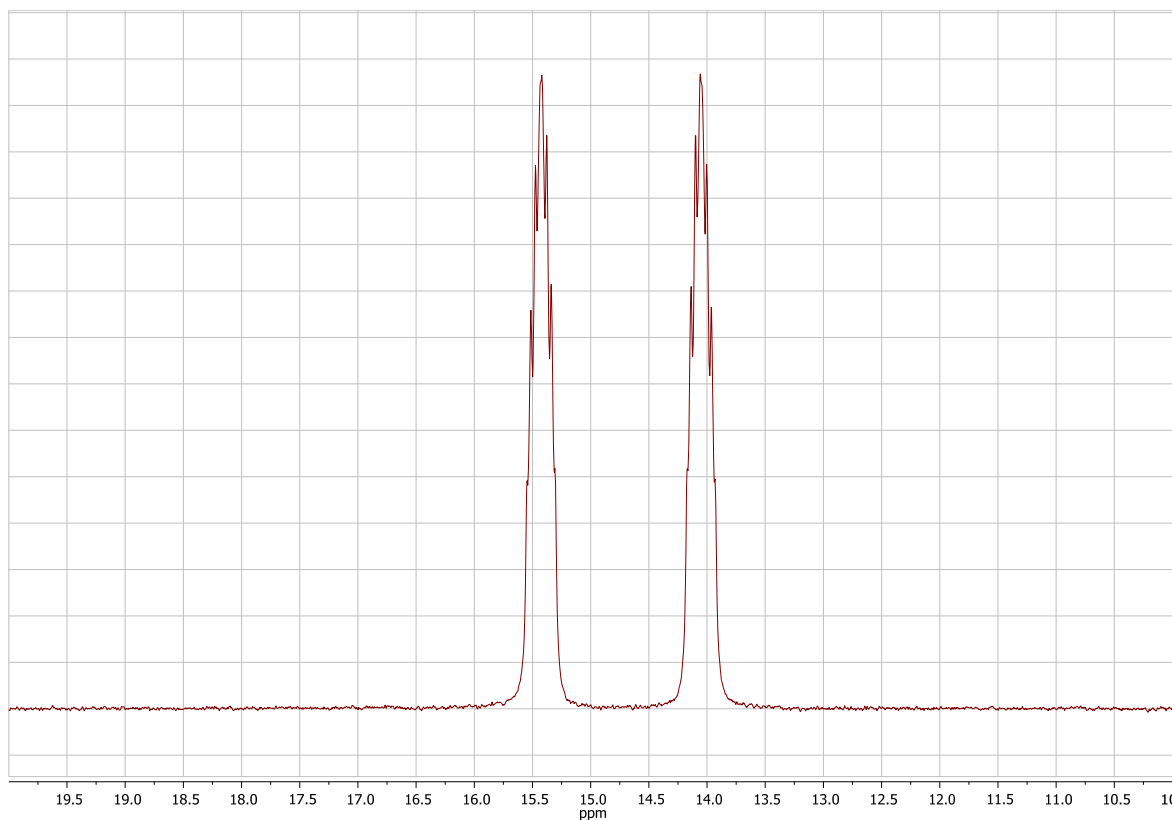


Figure S13. ^{109}Ag NMR spectrum of **2** dissolved in CD_3CN at room temperature (selected range).

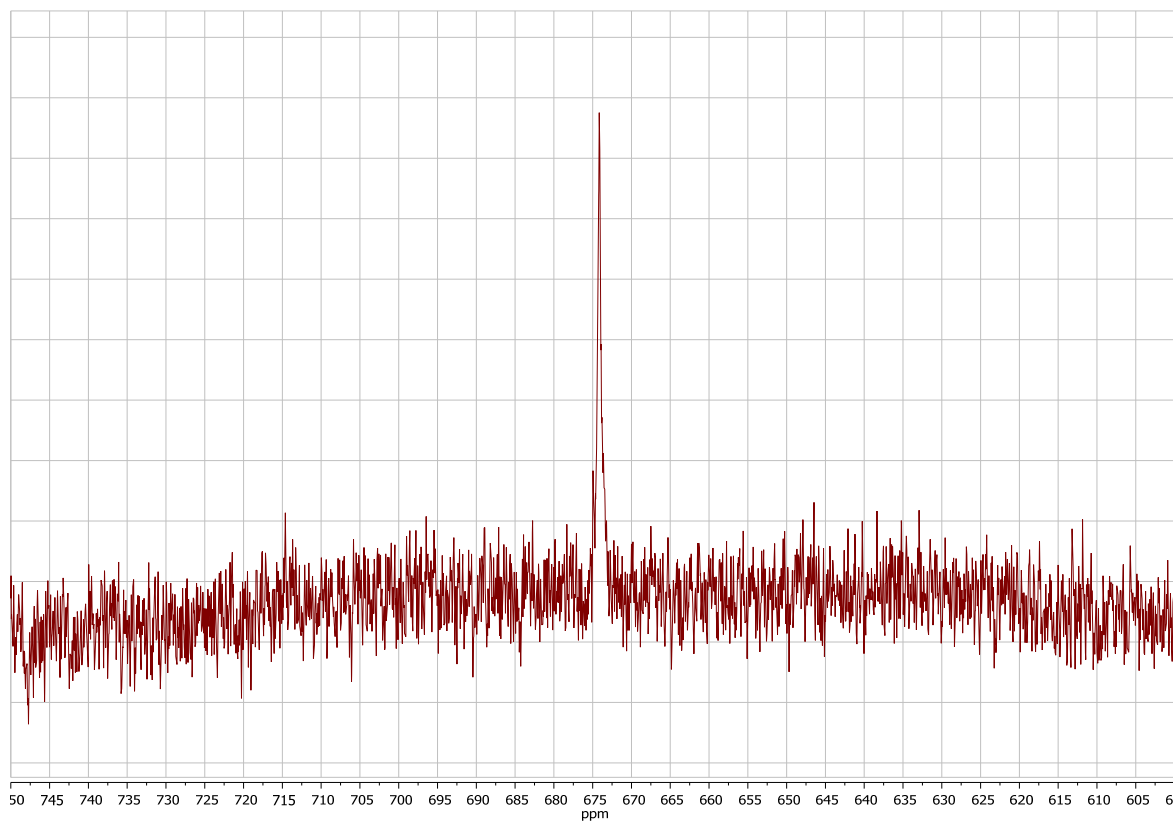


Figure S14. ^1H , ^{15}N -HMBC NMR spectrum of **2** dissolved in CD_3CN at room temperature (selected range).

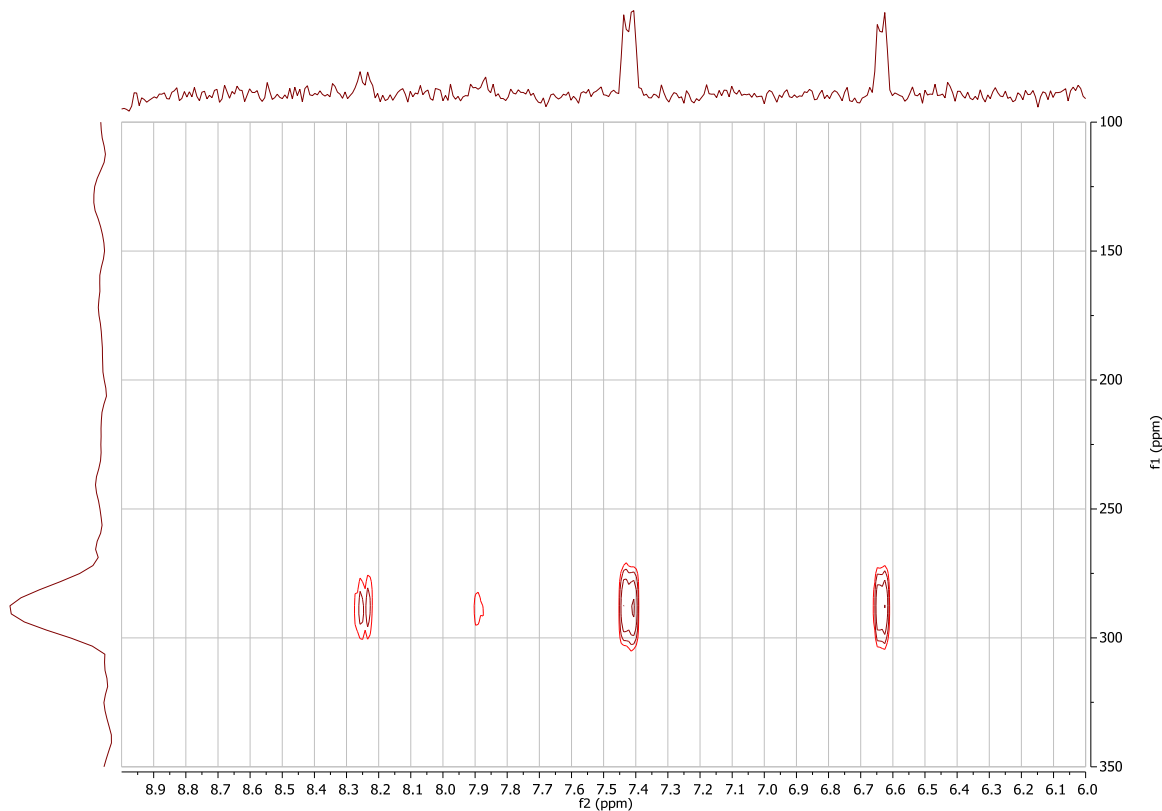


Figure S15. ^1H NMR spectrum of **3** dissolved in CD_3CN at room temperature (selected range).

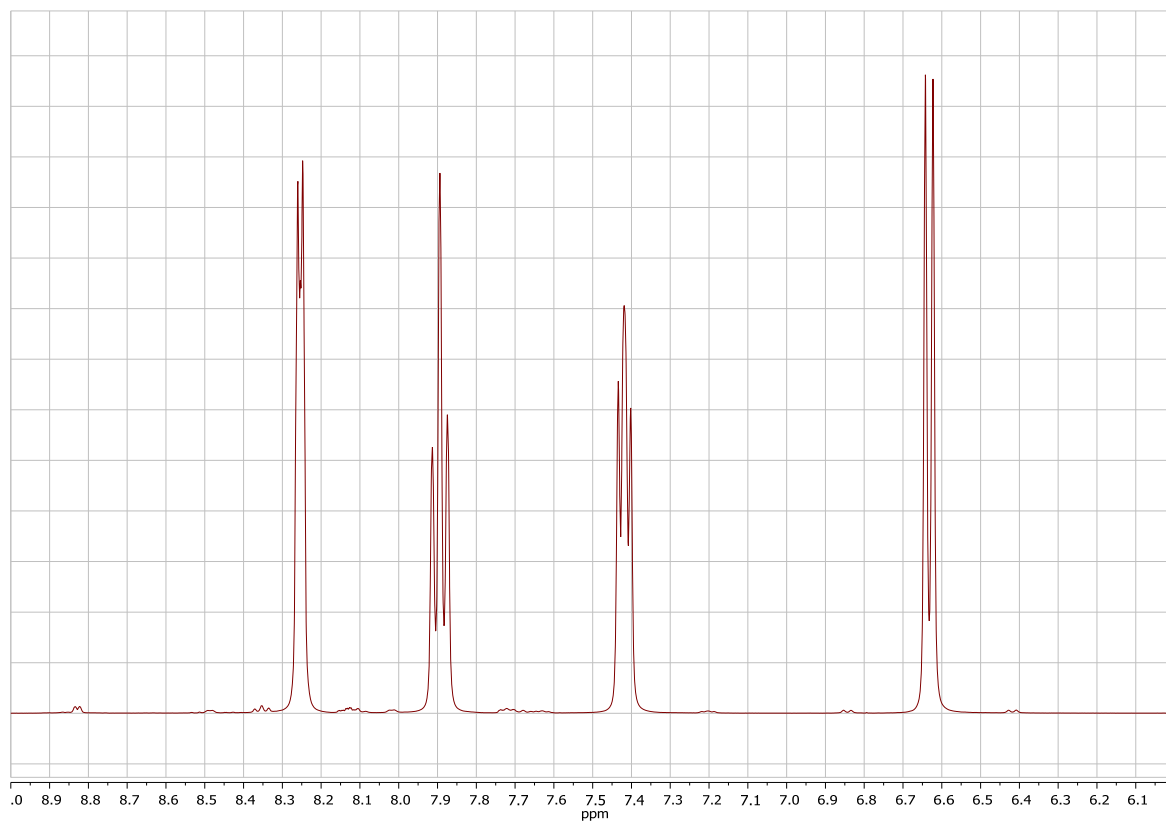


Figure S16. $^{31}\text{P}\{^1\text{H}\}$ NMR spectrum of **3** dissolved in CD_3CN at room temperature (selected range).

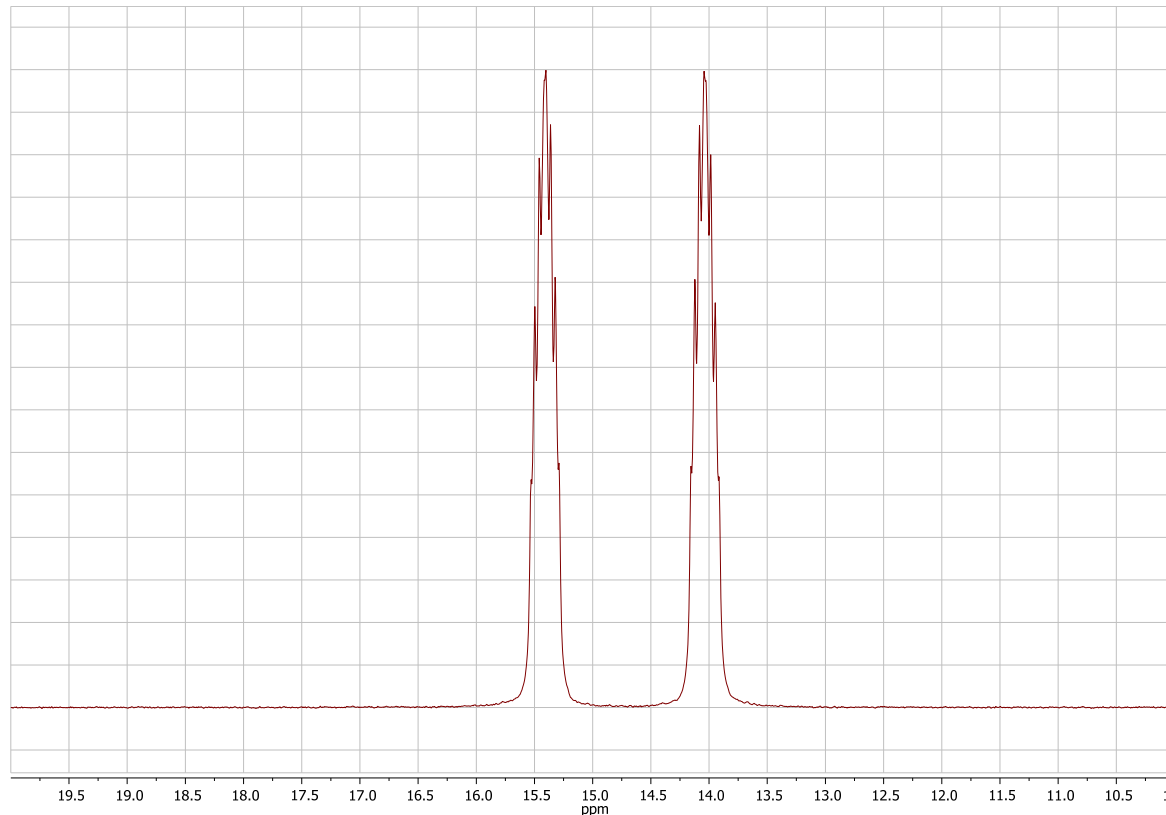


Figure S17. ^{109}Ag NMR spectrum of **3** dissolved in CD_3CN at room temperature (selected range).

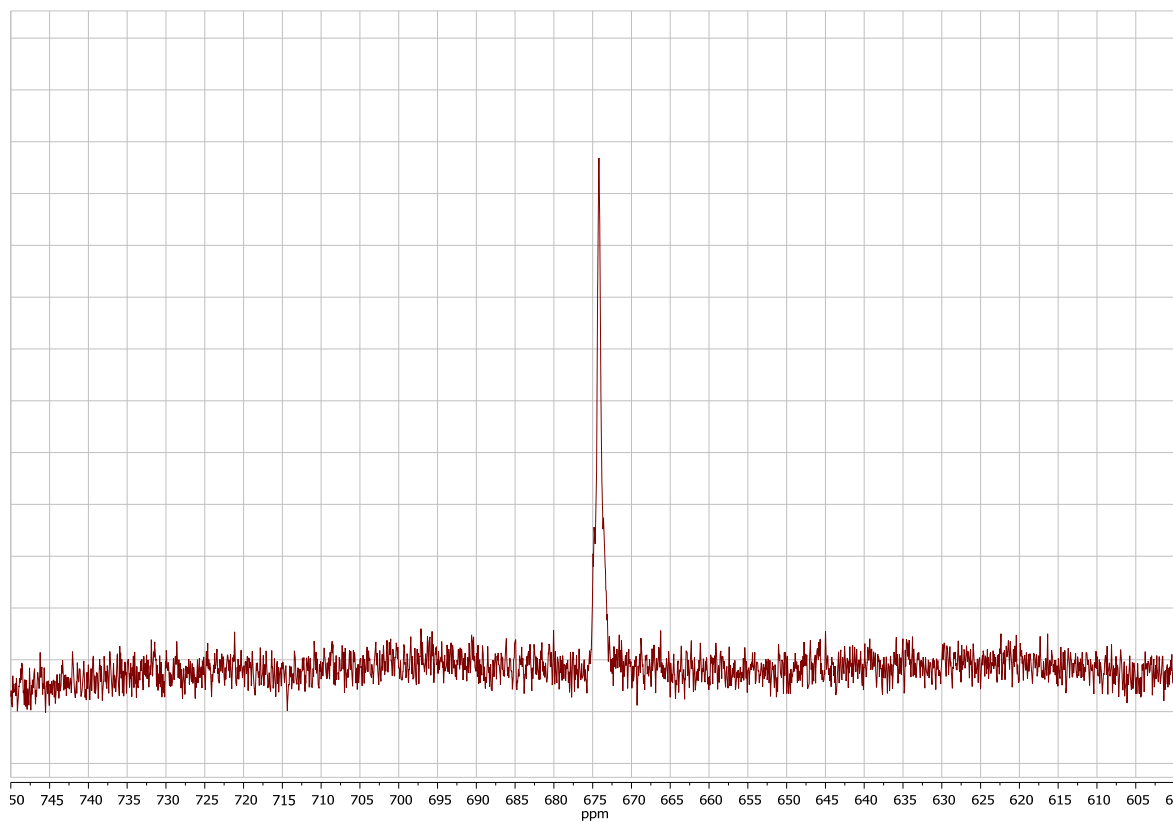


Figure S18. ^1H , ^{15}N -HMBC NMR spectrum of **3** dissolved in CD_3CN at room temperature (selected range).

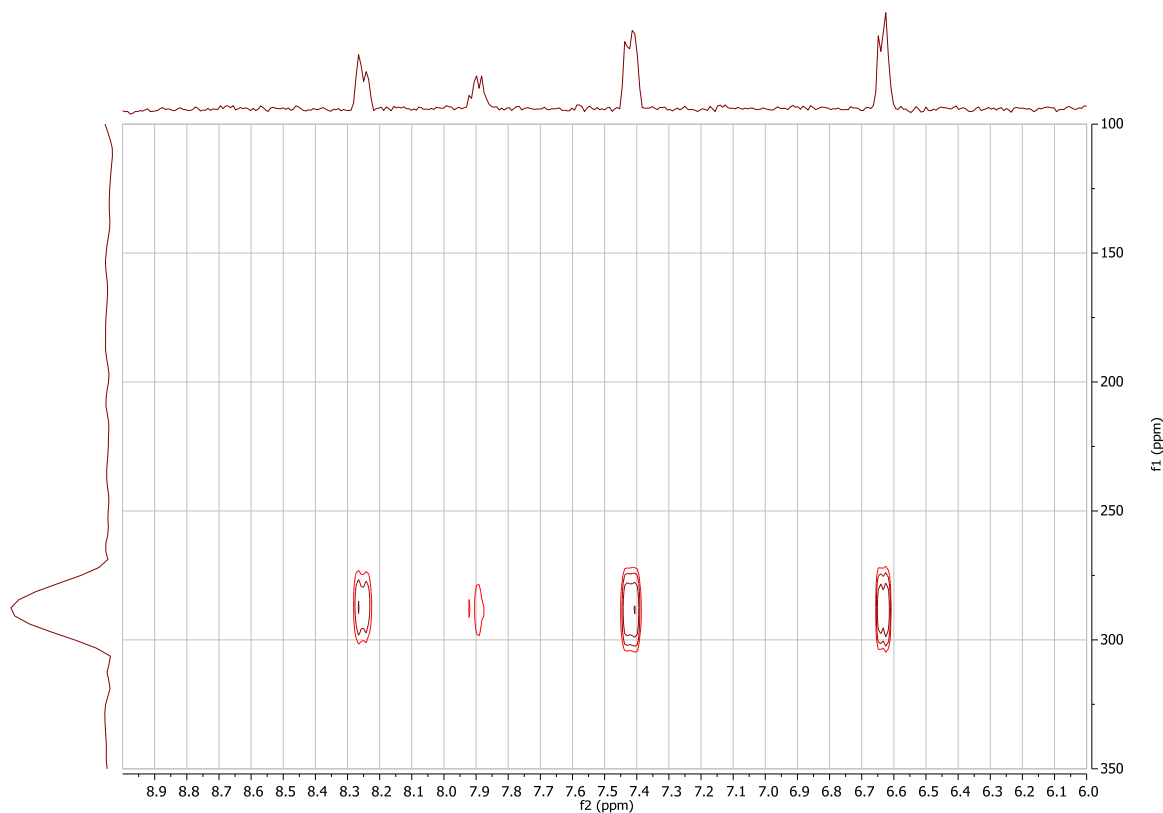


Figure S19. ^1H NMR spectrum of **4** dissolved in CD_3CN at room temperature (selected range).

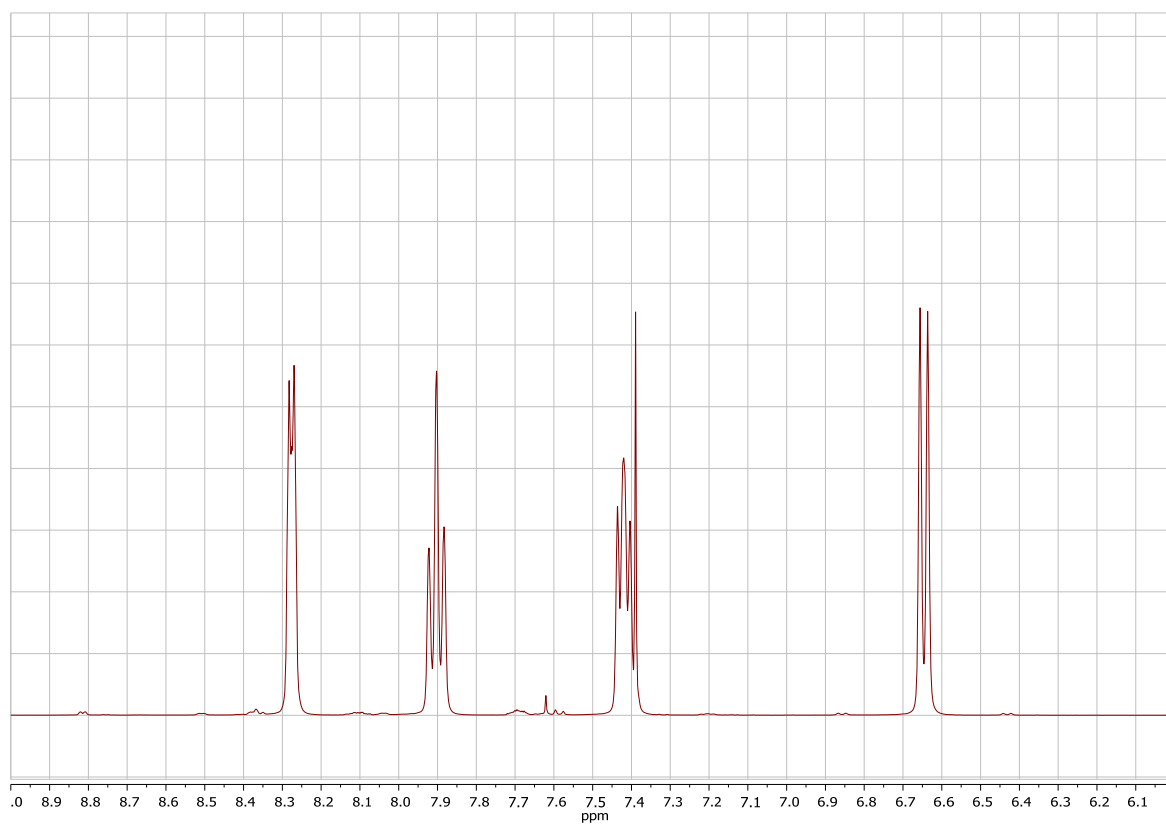


Figure S20. $^{31}\text{P}\{^1\text{H}\}$ NMR spectrum of **4** dissolved in CD_3CN at room temperature (selected range).

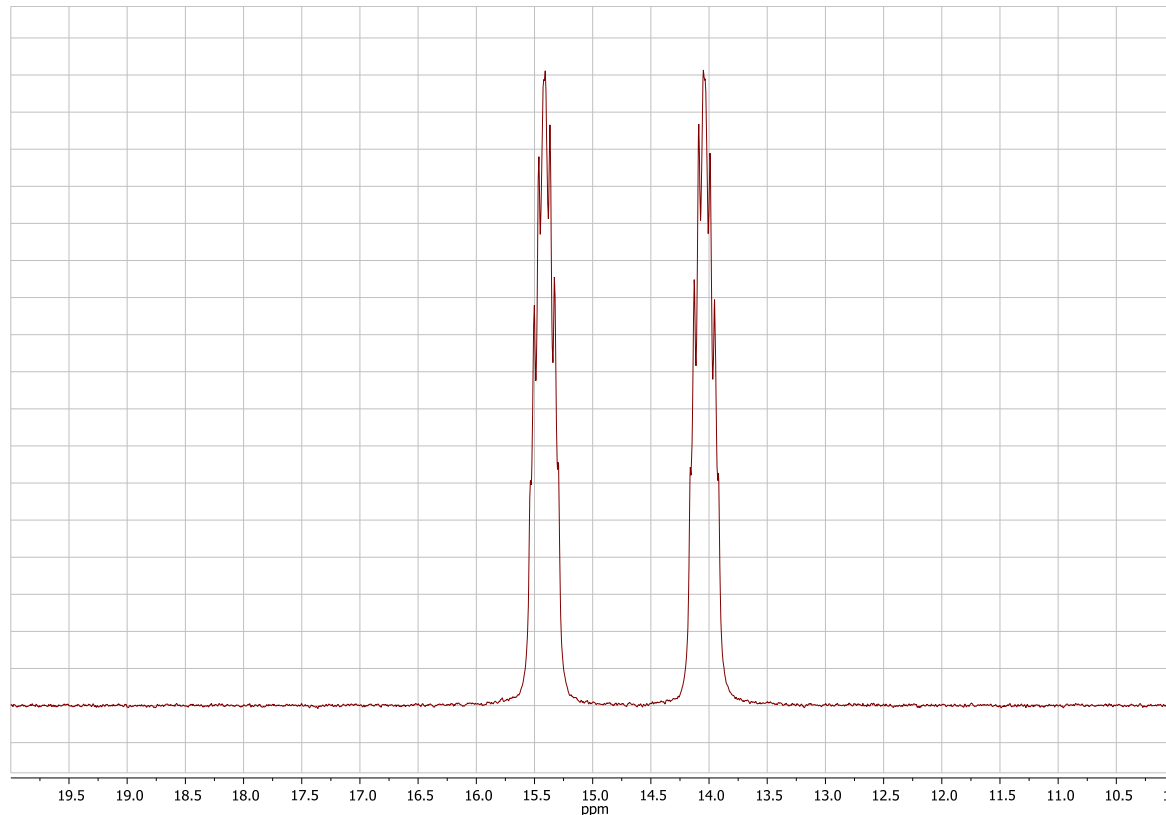


Figure S21. ^{109}Ag NMR spectrum of **4** dissolved in CD_3CN at room temperature (selected range).

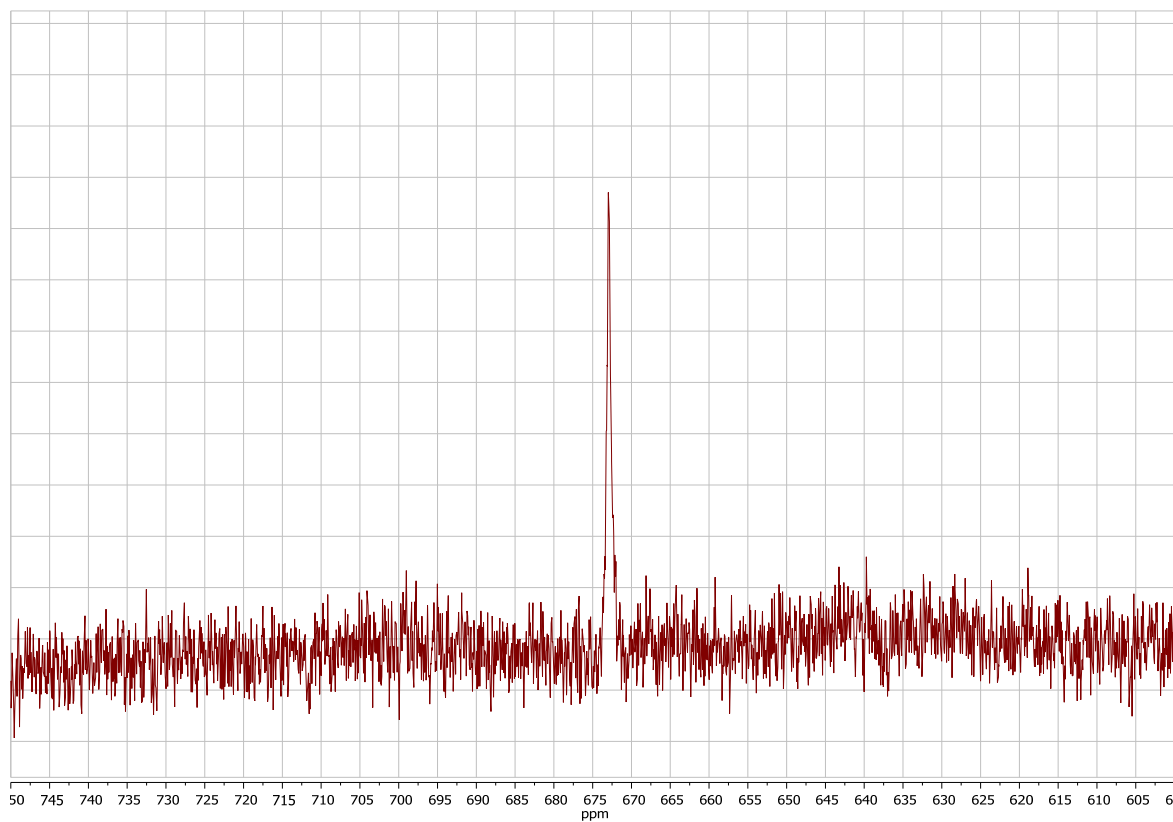


Figure S22. ^1H , ^{15}N -HMBC NMR spectrum of **4** dissolved in CD_3CN at room temperature (selected range).

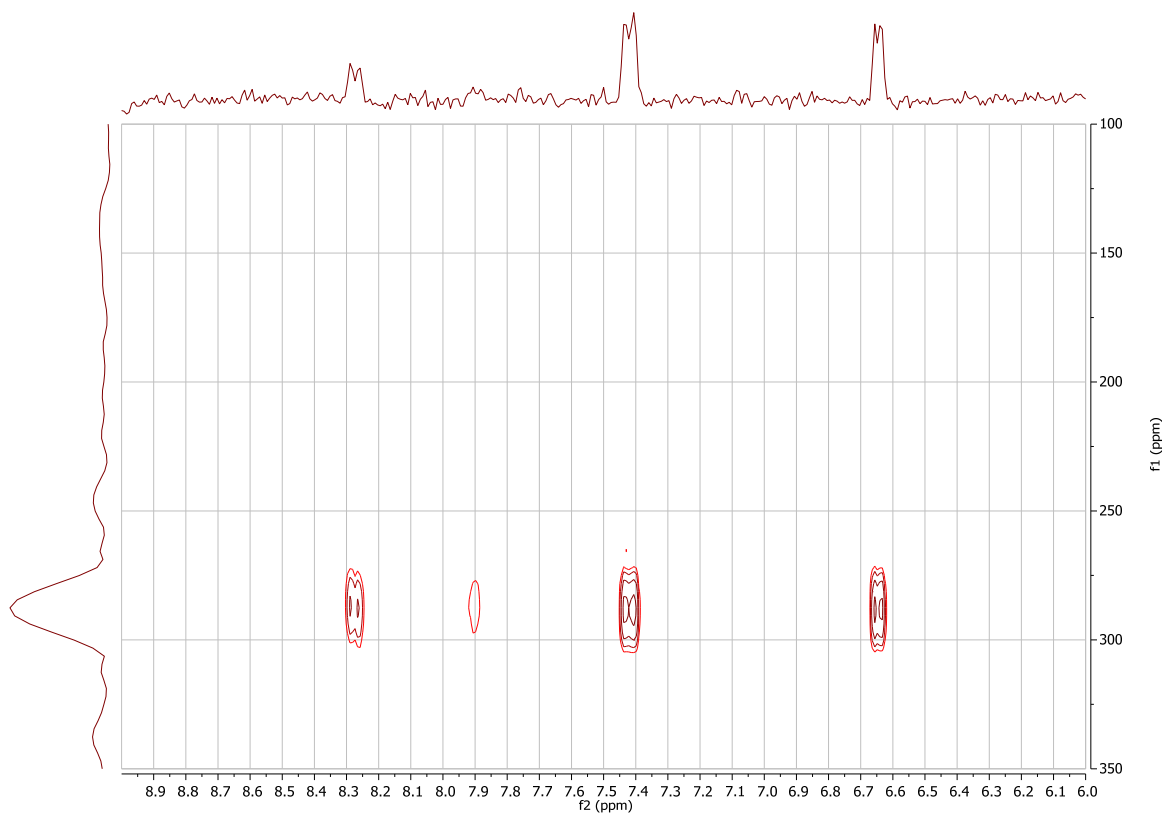


Figure S23. ^1H NMR spectrum of **5** dissolved in CD_3CN at room temperature (selected range).

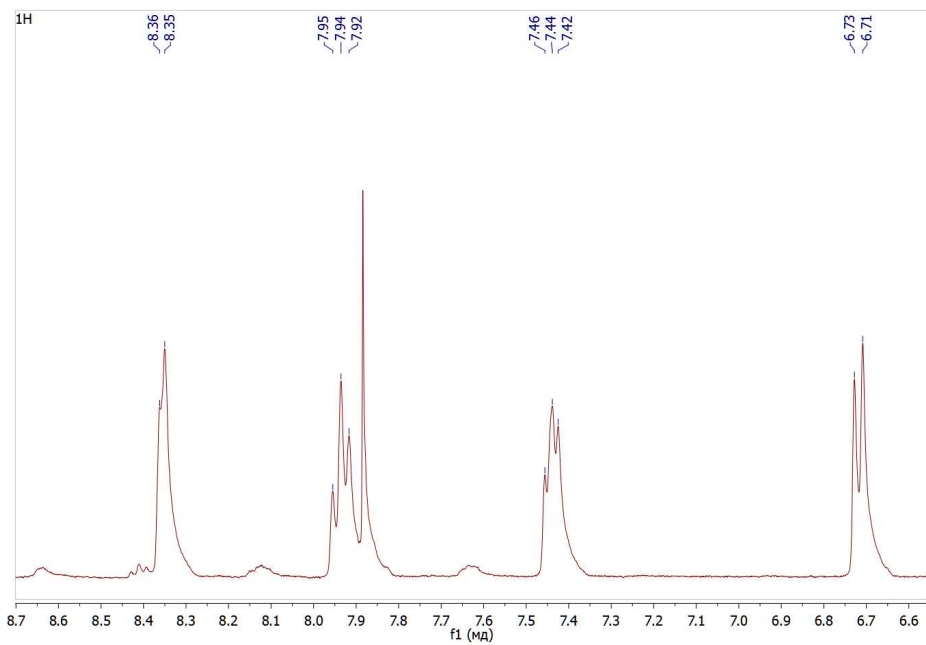
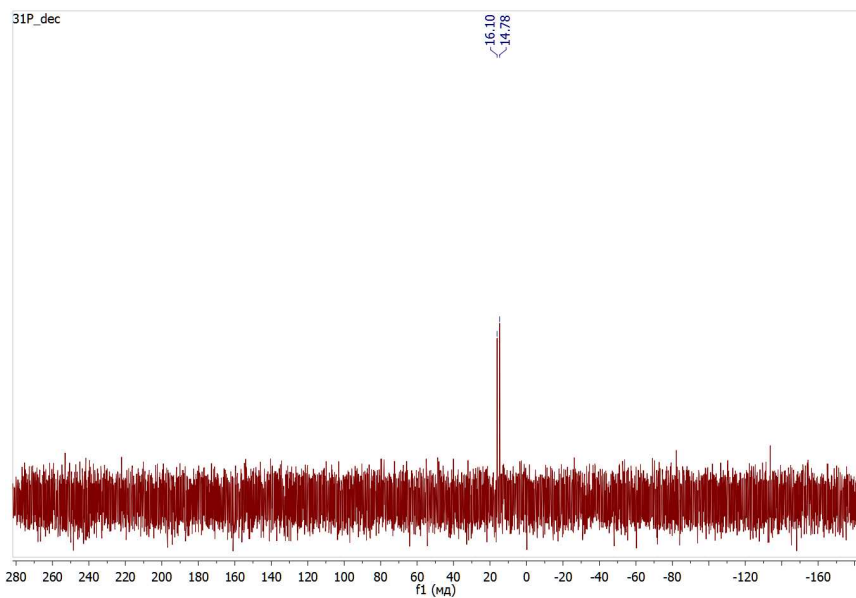


Figure S24. $^{31}\text{P}\{^1\text{H}\}$ NMR spectrum of **5** dissolved in CD_3CN at room temperature.



FT-IR spectra of the synthesized compounds 1-4

Figure S25. FTIR-ATR spectrum of 1.

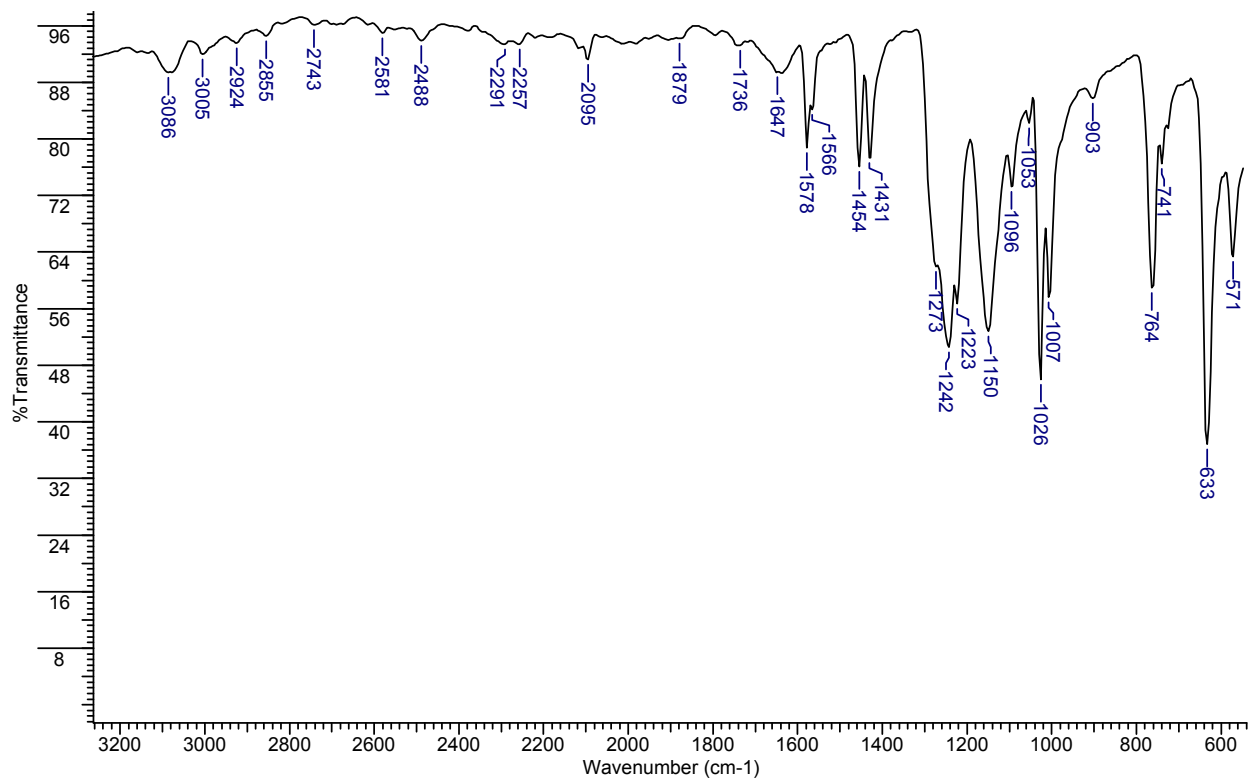


Figure S26. FTIR-ATR spectrum of 2.

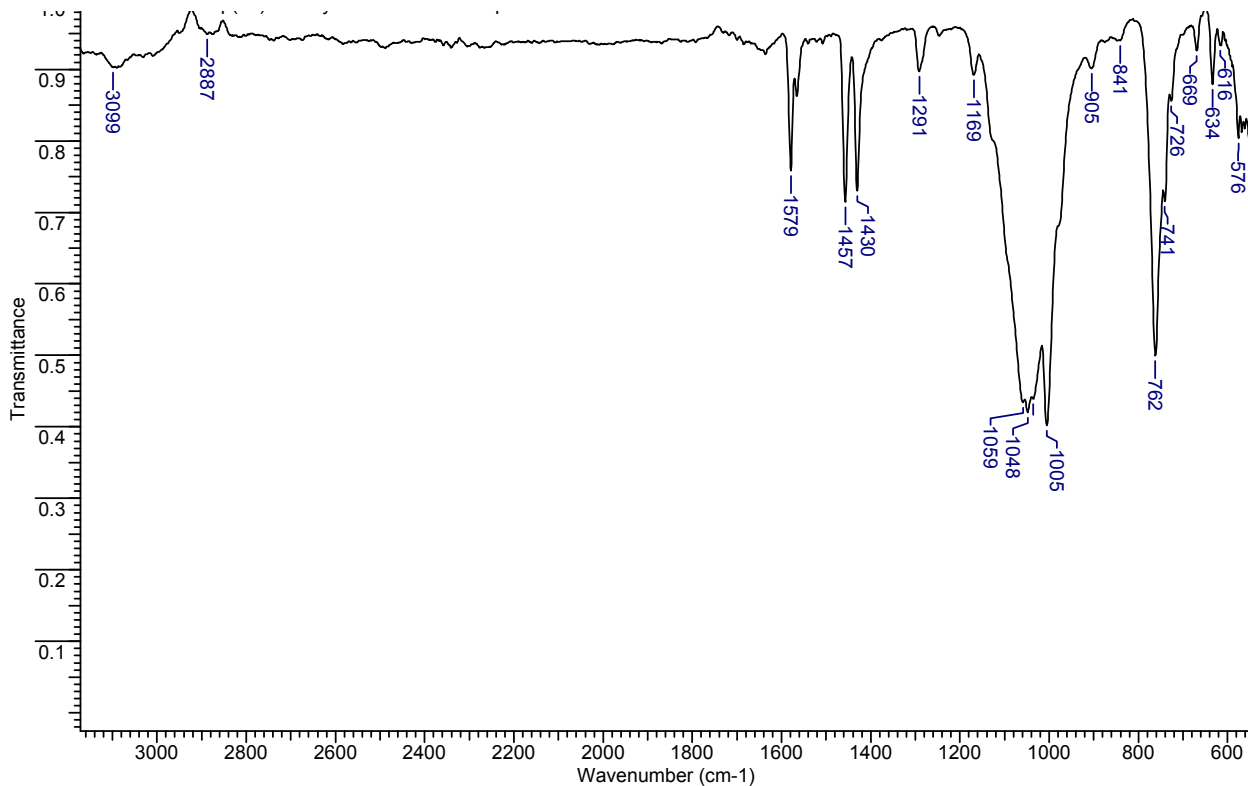


Figure S27. FTIR-ATR spectrum of **3**.

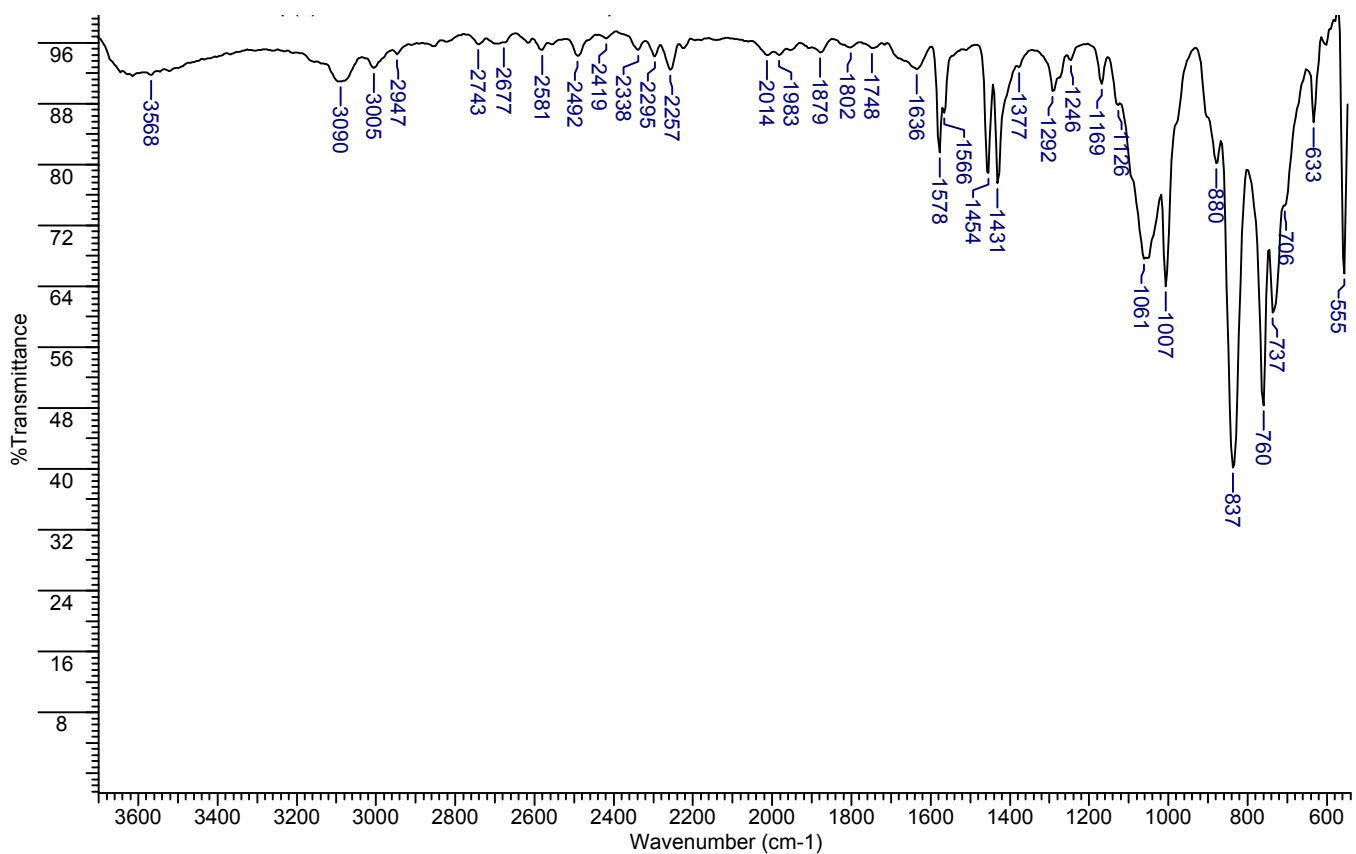
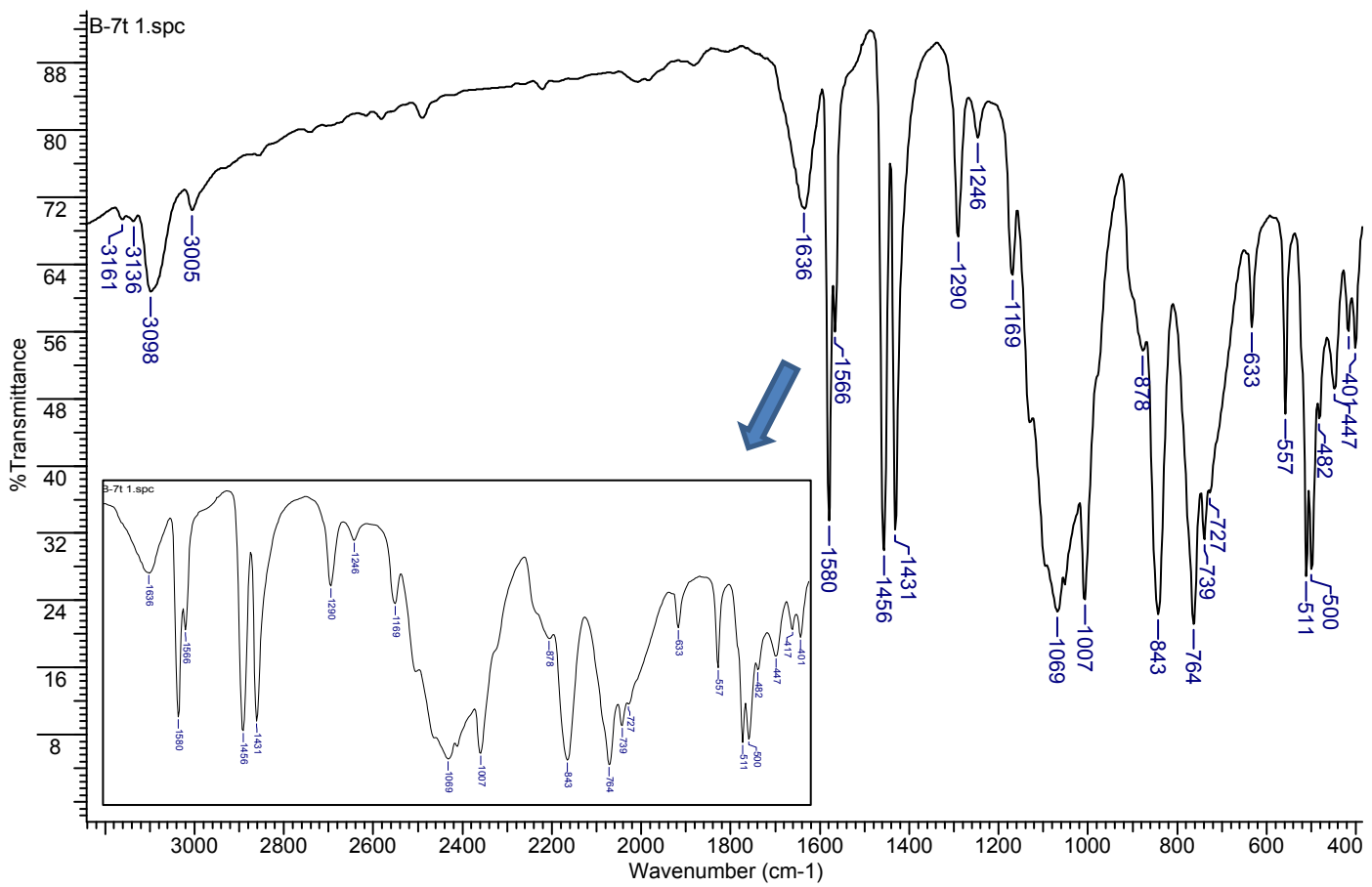


Figure S28. FTIR-ATR spectrum of 4.



Photophysical measurements

Excitation and emission spectra were recorded with a Horiba Jobin Yvon Fluorolog 3 photoluminescence spectrometer equipped with a 450 W Xe lamp, an integration sphere, Czerny–Turner double grating (1200 grooves per mm) excitation and emission monochromators and an FL-1073 PMT detector. Emission spectra were recorded from 360 to 700 nm and corrected for the spherical response of the monochromators and the detector using typical correction spectra provided by the manufacturer. Additionally, the 1st and 2nd harmonic oscillations of the excitation source were blocked by edge filters. The quantum yields were measured using a Quanta- ϕ Integrating sphere.

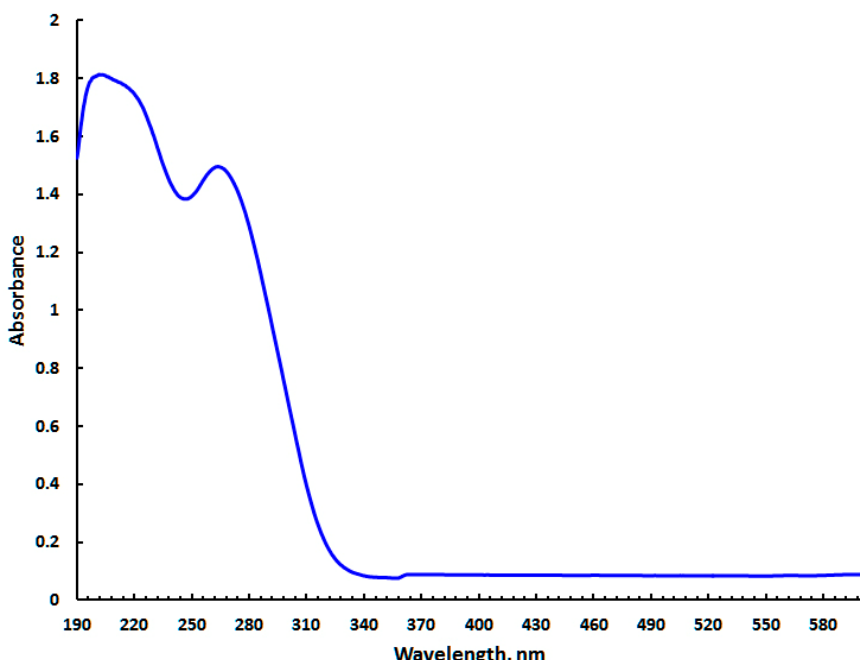
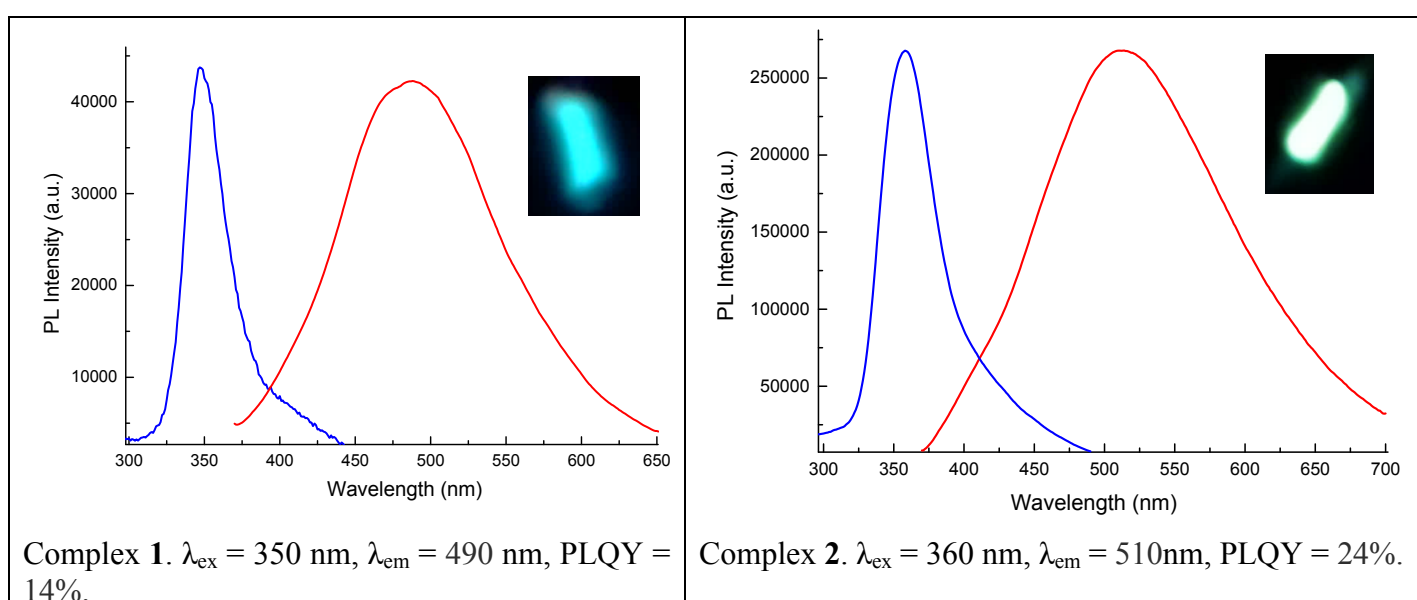
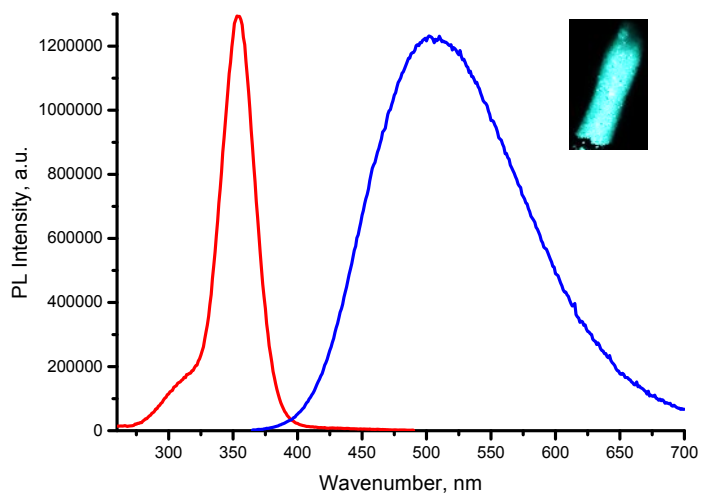
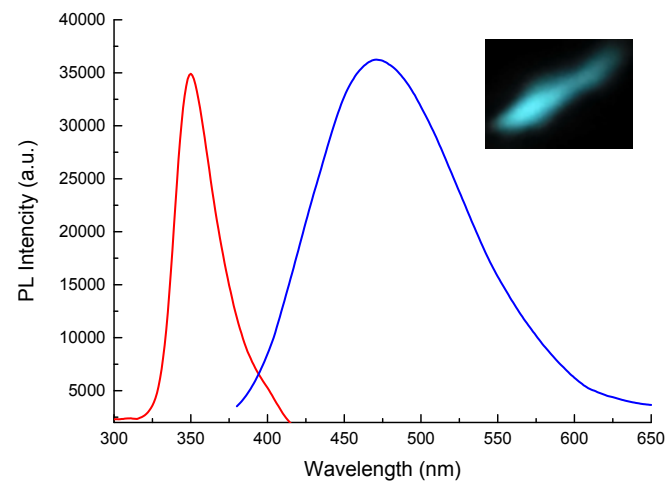
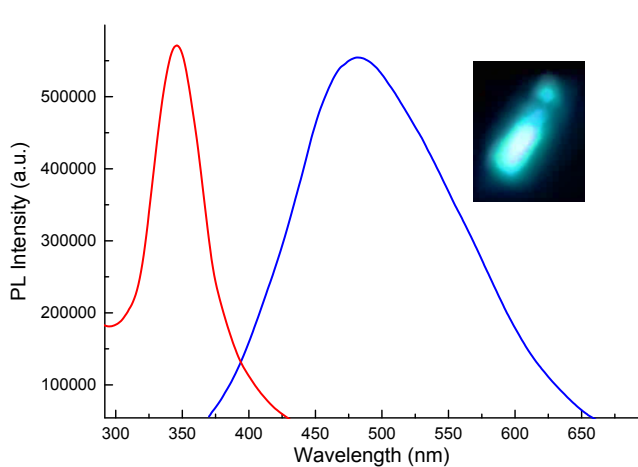


Figure S29. Typical UV-Vis spectrum for complexes **1-4** (MeCN, 300 K).

Figure S30. Normalized excitation and emission spectra of solid **1-5** (300 K).





CV measurements

The cyclic voltammograms (CV) were recorded with a 797 VA Computrace system (Metrohm, Switzerland). All measurements were performed with a conventional three-electrode configuration consisting of glassy carbon working and platinum auxiliary electrodes and an Ag/AgCl/KCl reference electrode. The solvent used in all experiments was CH₃CN which was deoxygenated before use. Tetra-n-butylammonium hexafluorophosphate (0.05 M solution) was used as a supporting electrolyte. The concentration of the cluster was approximately 1 mM.

Table S3. Cathodic potentials E_c (V, vs. Ag/AgCl) determined at the first and the second scans for **1-4** in the range from 0 to -2 V.

Compound	E _c (scan 1)	E _c (scan 2)
1	-1.2, -1.5	-0.77
2	-1.1, -1.7	-0.24, -0.65
3	-1.2, -1.5	-0.54
4	-1.3, -1.5	-0.69